

Forest-atmosphere exchange of reactive nitrogen in a remote region – Part II: Modeling annual budgets

Pascal Wintjen¹, Frederik Schrader¹, Martijn Schaap^{2,3}, Burkhard Beudert⁴, Richard Kranenburg², and Christian Brümmner¹

5 ¹Thünen Institute of Climate-Smart Agriculture, Bundesallee 68, 38116 Braunschweig, Germany

²TNO, Climate Air and Sustainability, Utrecht, 3584 CB, The Netherlands

³Institute of Meteorology, Freie Universität Berlin, 12165 Berlin, Germany

⁴Bavarian Forest National Park, 94481, Grafenau, Germany

Correspondence to: Pascal Wintjen (pascal.wintjen@thuenen.de)

10 **Abstract.** To monitor the effect of current nitrogen emissions and mitigation strategies, total (wet+dry) atmospheric nitrogen deposition to forests is commonly estimated using chemical transport models or canopy budget models in combination with throughfall measurements. Since flux measurements of reactive nitrogen (N_r) compounds are scarce, dry deposition process descriptions as well as the calculated flux estimates and annual budgets are subject to considerable uncertainties. In this study, we compared four different approaches to quantify annual dry deposition budgets of total reactive nitrogen (ΣN_r) at a mixed
15 forest site situated in the Bavarian Forest National Park, Germany. Dry deposition budgets were quantified based on (I) 2.5 years of eddy-covariance flux measurements with the Total Reactive Atmospheric Nitrogen Converter (TRANC), (II) an in-situ application of the bidirectional inferential resistance scheme DEPAC (Deposition of Acidifying Compounds), here called DEPAC-1D, (III) a simulation with the chemical transport model LOTOS-EUROS (Long Term Ozone Simulation – European Operational Smog) v2.0 using DEPAC as dry deposition module, and (IV) a canopy budget technique (CBT).
20 Averaged annual ΣN_r dry deposition estimates determined from TRANC measurements were 4.7 ± 0.2 and 4.3 ± 0.4 kg N ha⁻¹ a⁻¹ using DEPAC-1D only, and the Mean Diurnal Variation method in combination with DEPAC-1D as gap-filling approaches, respectively depending on the gap-filling approach. DEPAC-1D modeled dry deposition, using concentrations and meteorological drivers measured at the site, was 5.8 ± 0.1 kg N ha⁻¹ a⁻¹. In comparison to TRANC fluxes, DEPAC-1D estimates were systematically larger/higher during summer, and in close agreement in winter. Modeled ΣN_r deposition velocities (v_d) of
25 DEPAC-1D were found to increase with lower temperatures, higher relative humidity, and in the presence of wet leaf surfaces, in particular from May to September. This observation was in contradiction to TRANC-observed fluxes, leading to the conclusion that the parametrizations may need revision. LOTOS-EUROS modeled annual dry deposition was 6.5 ± 0.3 kg N ha⁻¹ a⁻¹ for the site-specific weighting of land-use classes within the site's grid cell. LOTOS-EUROS showed substantial discrepancies to measured ΣN_r deposition during spring and winter/autumn, which was related to an overestimation of ammonia
30 (NH_3) concentrations by a factor of two to three compared to measured values as a consequence of a mismatch between gridded input NH_3 emissions and the site's actual, rather low, pollution climate. within the grid cell. LOTOS-EUROS predicted an averaged ΣN_r concentration of 5.0 ± 3.3 $\mu\text{g N m}^{-3}$. According to LOTOS-EUROS predictions, ammonia (NH_3) contributed most to modeled input ΣN_r concentrations, whereas measurements showed NO_x as the prevailing compound in ΣN_r concentrations. but the modeled NH_3 concentrations were overestimated by a factor two to three compared to measured values.
35 Annual deposition estimates from measurements and modeling were in the range of minimum and maximum estimates determined from CBT being at 3.8 ± 0.5 and 6.7 ± 0.3 kg N ha⁻¹ a⁻¹, respectively. By adding locally measured wet-only deposition, we estimated an annual total nitrogen deposition input between 11.5 and 14.8 kg N ha⁻¹ a⁻¹, which is within the ~~at~~ the upper end of the critical load ranges proposed for deciduous and coniferous forests.
40 ~~In this work, we conducted one of the first comparisons of micrometeorological and ecological methods for estimating annual nitrogen dry deposition to a remote mixed forest.~~

1 Introduction

In the last century, global nitrogen emissions have increased significantly due to anthropogenic activities (Fowler et al., 2013). Reactive nitrogen compounds, such as ammonia (NH_3) and nitrogen oxides (NO_x), contribute most to the emissions. Ammonia emissions originate mostly from animal husbandry and fertilizer application (Sutton et al., 2011, 2013), whereas NO_x emissions are mainly related to combustion processes in, e.g., transport and industry (Erismann et al., 2011, 2013). Although fertilizer use and the internal combustion engine are vital for world's food security and the economy, the release of these compounds into the atmosphere has a wide range of negative effects (Krupa, 2003; Galloway et al., 2003; Erismann et al., 2013). Deposition of reactive nitrogen into ecosystems has been identified as a reduction factor for biodiversity (Bobbink et al., 1998; Krupa, 2003; Galloway et al., 2003; Sutton et al., 2011). Especially ecosystems ~~at~~ with nutrient poor soils are highly sensitive to additional nitrogen inputs resulting in a change in plant species (Damgaard et al., 2011; Paulissen et al., 2016) and species composition in forests (Dirnböck et al., 2014, 2018; Roth et al., 2022). Critical loads are used to show at which level ~~long~~ long-term nitrogen deposition may lead to adverse impacts (Hettelingh et al., 1995). Investigations by Hettelingh et al. (2013) have shown that half of the European ecosystems receive nitrogen above the critical ~~load~~ level. In Germany, the fraction of ecosystems with a critical load exceedance is estimated to be about 70 % (Schaap et al., 2018).

Quantitative estimation of the total nitrogen deposition is needed to assess exceedances of critical loads and to develop successful mitigation strategies. Although wet deposition is relatively straightforward to measure, the accurate quantification of dry N deposition remains a challenge. Recent progress in fast and robust measurement techniques allowed to investigate the temporal dynamics in concentrations and dry deposition fluxes (using the eddy-covariance (EC) approach) for total reactive nitrogen (ΣN_r) (Marx et al., 2012; Ammann et al., 2012; Brümmer et al., 2013, 2022; Zöll et al., 2019; Ammann et al., 2019; Wintjen et al., 2020, 2022) and its individual compounds, e.g. for NH_3 (Whitehead et al., 2008; Ferrara et al., 2012, 2021; Zöll et al., 2016; Moravek et al., 2020). For ΣN_r , the total reactive atmospheric nitrogen converter (TRANC) (Marx et al., 2012) coupled to a chemiluminescence detector (CLD) has shown its suitability for flux measurements in various field applications (see references for ΣN_r above). Despite the recent progress, the number and temporal coverage of available datasets remains small. -As these in-situ measurements are only valid for the ecosystem where the specific observations took place, a large-scale assessment based on observations alone is not ~~possible~~ feasible without a dense observation network.

Chemical transport models (CTMs) are used to assess nitrogen deposition over large regions. For Germany, the CTM LOTOS-EUROS (Wichink Kruit et al., 2012; Manders et al., 2017; van der Graaf et al., 2020) is applied for the mapping of nitrogen deposition fluxes across the country. LOTOS-EUROS predicts the dry deposition of various N_r compounds, namely nitrogen dioxide (NO_2), nitric oxide (NO), nitric acid (HNO_3), ammonia (NH_3), and particulate ammonium (NH_4^+) and nitrate (NO_3^-), in each grid cell by utilizing meteorological data from the European Centre for Medium Range Weather Forecasts (ECMWF), modeled concentrations of the mentioned compounds based on their emission sources and chemical processing, as well as information about the land-use distribution within each grid cell. The deposition module DEPAC (Deposition of Acidifying Compounds) is applied for calculating dry deposition velocities of those compounds (Erismann et al., 1994). DEPAC is a dry deposition inferential scheme featuring bidirectional NH_3 exchange (van Zanten et al., 2010; Wichink Kruit et al., 2012), which is also implemented in the Operational Priority Substance (OPS) model (van Jaarsveld, 2004; Sauter et al., 2020). DEPAC can be used as stand-alone model for estimating dry deposition of N_r compounds. For site-based modeling with DEPAC, decoupled from a CTM and henceforth called DEPAC-1D, only measurements of common micrometeorological variables and concentrations of the individual N_r compounds are needed. In the past, deposition estimates have often been obtained through such an inferential modeling approach (Flechard et al., 2011, 2020; Li et al., 2016; Schwede et al., 2011).

To evaluate modeled annual total dry deposition and seasonal patterns in modeled fluxes and deposition velocities, a careful comparative analysis to flux measurements may provide feedback on the representativeness of the input data and the bidirectional parametrizations (Wichink Kruit et al., 2010; Wichink Kruit et al., 2017). Wintjen et al. (2022) presented and analyzed novel flux measurements of ΣN_r and several subcomponents ~~focussing~~ focusing on temporal dynamics above a remote, mixed forest site spanning a 2.5-year period. This dataset provides a unique opportunity for the evaluation of different approaches to quantify dry deposition fluxes. Such comparisons with novel measurement techniques are sparse and only available from few field campaigns (Ammann et al., 2012; Brümmer et al., 2013, 2022; Zöll et al., 2019). Since the adoption of the Geneva Convention on Long-Range Transboundary Air Pollution (CLRTAP) in 1979, throughfall measurements have been carried out at many sites of the International Co-operative Programmes on Assessment and Monitoring of Air Pollution Effects on Forests (ICP Forests, www.icp-forests.net, last access: 14 March 2022) and forested catchments (ICP Integrated Monitoring, <http://www.syke.fi/nature/icpim>, last access: 14 March 2022) according to standardized protocols. Using the so-called canopy budget technique (CBT), throughfall measurements also allow to give an estimate of the annual nitrogen dry deposition (Draaijers and Erisman, 1995; de Vries et al., 2003).

In this study, we provide a comparison of four independent methods for estimating nitrogen dry deposition for a remote mixed forest site in the Bavarian Forest National Park. The comparison is made for a 2.5-year period for which novel flux measurements were available (see companion paper Wintjen et al., 2022). The aim of this measurement campaign covering the time frame from January 2016 to June 2018 was to quantify background concentration and deposition levels as well as their temporal dynamics for further improvements in modeling nitrogen deposition that may be used for further defining environmental protection guidelines. Therefore, (1) we present modeled concentrations, deposition velocities, and fluxes of ΣN_r and compare them to measurements of the same ~~variables~~ compounds (1), (2) discuss the influence of micrometeorological parameters on modeled deposition velocities ~~of ΣN_r~~ and the impact of measured and modeled input parameters on modeled ~~NH_3~~ fluxes (2), and (3) compare annual N_r budgets of LOTOS-EUROS with DEPAC-1D, flux measurements, and nitrogen deposition estimates based on CBT and reviewing them in the context of critical loads (3) and (4) finally discuss uncertainties affecting modeled dry deposition estimates.

2 Materials and Methods

2.1 ~~Site and campaign description~~ Data set description

~~The campaign took place at a remote location in the Bavarian Forest National Park (NPBW) (48° 56' N 13° 25' E, 807 m a.s.l.), a natural mixed forest located close to the Czech Border in the southeast of Germany. Due to the absence of nearby anthropogenic emission hotspots in terms of intensive agriculture or industry, concentrations of air pollutants are at background concentration level (Beudert and Breit, 2010). Observations of air pollutants and micrometeorology started on a 50 m tower in the 1980s. The measurement site is located in the Forellenbach catchment (Beudert and Gietl, 2015). The Forellenbach site is part of several networks for monitoring air pollution, e.g., International Cooperative Program on Integrated Monitoring of Air Pollution Effects on Ecosystems (ICP-IM) within the framework of the Geneva Convention on Long-Range Transboundary Air Pollution (UNECE, 2022) and Long-Term Ecological Research (LTER, 2022). The Federal Environment Agency (UBA) and the NPBW Administration are responsible for the contribution to these networks. Further details about the site can be found in Zöll et al. (2019) and Wintjen et al. (2022).~~

~~For the application of DEPAC-1D, time series of micrometeorological parameters (i.e. temperature, atmospheric pressure, relative humidity, global radiation, Obukhov length, friction velocity) and air pollutant concentrations (NO , NO_2 , HNO_3 , NH_3 , NO_3^- , NH_4^+ , and sulphur dioxide (SO_2)) are required for the flux calculations. These concentration measurements were~~

125 performed using a DELTA (DENuder for Long-Term Atmospheric sampling e.g., Sutton et al., 2001; Tang et al., 2009) system
 installed at 30 m above the forest floor. NH₃ was additionally collected by passive samplers of the IVL type (Ferm, 1991) at
 several levels from the ground to 50 m including 30 m. In addition, high resolution measurements of NH₃ were made with a
 Quantum Cascade Laser (QCL) (model mini QC TILDAS 76 from Aerodyne Research, Inc. (ARI, Billerica, MA, USA)). The
 setup was completed by the TRANC integrated in an EC system consisting of a sonic anemometer (GILL R3, Gill Instruments,
 130 Lymington, UK) and a chemiluminescence detector (CLD 780 TR, ECO PHYSICS AG, Dürnten, Switzerland). This system
 allowed flux measurements of ΣN_r and common micrometeorological parameters. All instruments were installed at 30 m except
 for the CLD, which was placed in an air-conditioned box at the ground and connected to the TRANC via a 45 m opaque PTFE
 sampling line. NO, NO₂, and further meteorological parameters including pressure and global radiation were observed by the
 NPBW at 50 m. Profile measurements of relative humidity and temperature were made at 10 m, 20 m, 40 m, and 50 m height.
 135 All devices installed at the site as well as the TRANC are described in Wintjen et al. (2022).

For the comparison to modeled ΣN_r deposition fluxes, TRANC EC flux measurements described in detail in Wintjen et al
 (2022) were used. These flux measurements were available at half-hourly resolution, carried out 30 m above the forest floor,
 and had a data coverage of 41.0 % considering the entire campaign period. Data gaps were related to violations of the EC
 140 theory and performance issues of the instruments.

For the application of DEPAC-1D, time series of micrometeorological parameters (i.e. temperature, atmospheric pressure,
 relative humidity, global radiation, Obukhov length (L), friction velocity (u_*) and air pollutant concentrations (NO, NO₂,
 HNO₃, NH₃, pNO₃⁻, pNH₄⁺, and sulphur dioxide (SO₂)) are required for flux calculations. NH₃ concentrations obtained from
 Quantum cascade laser measurements taken at 30 m above ground, NO₂ and NO obtained from chemiluminescence
 145 measurements taken at 50 m above ground as well as micrometeorological parameters were aggregated at half-hourly
 resolution, whereas the remaining N_r species and an additional NH₃ determination were obtained from DELTA (DENuder for
 Long-Term Atmospheric sampling, e.g., Sutton et al., 2001; Tang et al., 2009) and passive sampler (NH₃ only) measurements
 of the IVL type (Ferm, 1991) for on monthly basis. DELTA measurements were made at 30 m and passive sampler
 measurements at 10, 20, 30, 40, and 50 m above ground. Temperature and relative humidity were collected in a profile at 10,
 150 20, 40, and 50 m above ground. Pressure and global radiation measurements were taken at 50 m. Indicators of stability and
 turbulence such as L and u_* were obtained from momentum flux measurements of the sonic anemometer.

Gaps in DEPAC-1D were related to gaps in micrometeorological input data and issues in the measurements of N_r compounds.
 Respective half-hourly values in the flux time series of each gas (approx. 3.4% for NH₃, HNO₃, pNH₄⁺, and pNO₃⁻ and 9.3%
 155 for NO and NO₂) were filled with results from LOTOS-EUROS. A detailed description of the site and the instrumentation is
 given in Wintjen et al. (2022). For LOTOS-EUROS flux modeling, modeled input data of the European Centre for Medium
 range Weather Forecast (ECMWF) and the national emission inventory of Germany (Schneider et al., 2016) were used to
 predict deposition fluxes for NO, NO₂, HNO₃, NH₃, pNO₃⁻, and pNH₄⁺. LOTOS-EUROS fluxes were resampled to half-hourly
 timestamps from the original hourly resolution and missing fluxes were linearly interpolated. For the canopy budget technique,
 160 throughfall measurements under spruce and beech trees in close proximity to the station (Beudert et al., 2014) and bulk
 deposition measurements at an open site (Wintjen et al., 2022) were taken in weekly intervals and used for determination of
 total nitrogen dry deposition on annual basis (Sect. 2.3). An overview of all methods is given in Table 1.

Table 1 Overview of methods used for estimating ΣN_r dry deposition.

Method	Primary input/observation variables and temporal resolution	Primary output variables and temporal resolution
--------	---	--

TRANC	Wind components (u, v, w), sonic temperature (T_s), and ΣN_r concentration at 10 Hz resolution	ΣN_r fluxes at half-hourly resolution, no gap-filling applied
DEPAC-1D	Measurements of micrometeorological variables at half-hourly resolution Measured NH_3 , NO , NO_2 concentrations at half-hourly resolution Measured SO_2 , HNO_3 , NH_3 , pNO_3^- , and pNH_4^+ concentrations at monthly resolution	Fluxes of NH_3 , NO_2 , NO , HNO_3 , pNH_4^+ , and pNO_3^- at continuous half-hourly resolution
TRANC (DEPAC-1D)	See above	Continuous ΣN_r fluxes at half-hourly resolution, only DEPAC-1D is used for gap-filling
TRANC (MDV+DEPAC-1D)	See above	Continuous ΣN_r fluxes at half-hourly resolution, gap-filled with a combination of MDV (window size of ± 5 days) and DEPAC-1D for adding further missing fluxes
LOTOS-EUROS	Meteorological data from ECMWF weather forecasts and modeled concentrations of SO_2 , NH_3 , NO_2 , NO , HNO_3 , pNH_4^+ , and pNO_3^- at hourly resolution for 7×7 km ² grid cell; concentrations were linearly resampled to half-hourly resolution	Continuous fluxes of NH_3 , NO_2 , NO , HNO_3 , pNH_4^+ , and pNO_3^- at hourly resolution; fluxes were linearly resampled to half-hourly resolution
Canopy budget technique	Throughfall measurements from nearby spruce and beech trees and bulk deposition measurements at an open-site in weekly intervals	Dissolved inorganic nitrogen deposition (DIN) based on the exchange of NO_3^- and NH_4^+ ions on monthly basis following the approaches of Draaijers and Erismann (1995) and de Vries et al. (2003), dissolved organic nitrogen (DON) corresponds to difference of DON fluxes between throughfall and bulk deposition

165

To compare dry deposition estimates from modeling to TRANC measurements, we filled gaps in the TRANC flux data with results from DEPAC-1D and henceforth, called this dataset TRANC(DEPAC-1D). In a second approach, we applied the mean-diurnal-variation (MDV) method to short-term gaps analogous to Wintjen et al. (2022) and replaced remaining gaps with results from DEPAC-1D. This approach was called TRANC(MDV+DEPAC-1D). Both approaches, DEPAC-1D alone and the

170 combination of DEPAC-1D and MDV, were able to fill all gaps in TRANC flux time series. Uncertainties of the gap-filled
 175 fluxes determined by MDV were calculated as the standard error of the mean. Cumulative uncertainties of TRANC fluxes
 were solely based on the uncertainty of the gap-filling and were calculated according to Eq. (3) of Wintjen et al. (2022). The
 error calculation scheme proposed by Brümmer et al. (2022, Eq. (1)) was applied to fluxes filled with DEPAC-1D. Flux
 uncertainty of those half-hourly values was given as

$$F_{\text{unc,DEPAC-1D}} = \frac{\tilde{X}}{F_{\text{DEPAC-1D}}} ; \text{ with } \tilde{X} = \frac{F_{\text{unc,meas}}}{F_{\text{meas}}} \quad (1)$$

175 where \tilde{X} represents the median of the ratio of the uncertainty of the measured fluxes ($F_{\text{unc,meas}}$) to their corresponding flux
 values (F_{meas}). The uncertainty of the measured fluxes was estimated after Finkelstein and Sims (2001). Systematic
 uncertainties were not accounted in the error calculation. A discussion on systematic uncertainties is given in Wintjen et al.
 (2022).

180

2.2 Modeling reactive nitrogen fluxes

2.2.1 Bidirectional resistance model DEPAC

In surface-atmosphere exchange models, fluxes are calculated by using resistance schemes. In case of gases exhibiting
 bidirectional exchange behavior, the flux F is defined as follows

$$F = -v_d(z-d) \cdot (\chi_a(z-d) - \chi_{\text{tot}}) \quad (2)$$

185 The flux is a product of the deposition velocity (v_d) with the concentration difference between the atmospheric concentration
 and the compensation point of the trace gas χ_a . In DEPAC, a compensation point is only implemented for NH_3 . Both, the dry
 deposition or exchange velocity ~~as~~ and the atmospheric concentration, are height dependent and given for an aerodynamic
 reference height ($z-d$) where z is the geometric height and d the zero-plane displacement height. The following convention is
 used for the fluxes: negative values represent deposition, positive values emission. Following the conductivity-resistance
 190 analogy, v_d is the inverse of the sum of the aerodynamic resistance (R_a), the quasi-laminar layer resistance (R_b), and the canopy
 resistance (R_c).

$$v_d = (R_a + R_b + R_c)^{-1} \quad (3)$$

DEPAC (van Zanten, et al., 2010) can be used to calculate the dry deposition of reactive nitrogen gases. ~~The aerodynamic~~
~~(R_a) and laminar layer (R_b) resistances~~ are required by DEPAC as input variables. Hence, the module is oriented at determining
 R_c for NO , NO_2 , HNO_3 , and NH_3 . R_c is treated differently for each N_r compound but basically as the sum of parallel resistances,
 195 which model the exchange behavior of the atmosphere and vegetation:

$$R_c^{-1} = R_w^{-1} + R_{\text{stom}}^{-1} + (R_{\text{inc}} + R_{\text{soil}})^{-1} \quad (4)$$

The stomatal resistance (R_{stom}) is calculated following Emberson et al. (2000a, b). In this scheme, stomatal conductance is
 determined by vegetation type dependent on maximum conductance lowered by factors controlling stomatal opening, i.e. light
 intensity, ambient temperature, vapor pressure deficit, and soil water content, using well known Jarvis functions (Jarvis, 1976).
 200 For NH_3 a stomatal compensation point (χ_{stom}) is calculated following Wichink Kruit et al. (2010, 2017). The cuticular
 resistance (R_w) is described by Sutton and Fowler (1993) for NH_3 and the corresponding cuticular compensation point based

on the works of Wichink Kruit et al. (2010, 2017). For NO and NO₂, R_w is set considerably high to 10000 and 2000 s m⁻¹, respectively, allowing hardly any deposition on external surfaces. The in-canopy resistance (R_{inc}) is given by van Pul and Jacobs (1994), and the soil resistance (R_{soil}) is described following Erismann and van Pul (1994). In the current version of
 205 DEPAC, the soil compensation point is set to zero for all surface types. In case of HNO₃, a fast uptake to any surface is assumed through a low, constant R_c of 10 s m⁻¹. The total compensation point (χ_{tot}) is determined as written in van Zanten et al. (2010).

$$\chi_{tot} = \frac{R_c}{R_w} \cdot \chi_w + \frac{R_c}{R_{inc} + R_{soil}} \cdot \chi_{soil} + \frac{R_c}{R_{stom}} \cdot \chi_{stom} \quad (54)$$

For further details to the documentation of DEPAC, we refer to the publication of van Zanten et al. (2010). Following implementation in LOTOS-EUROS, the version of DEPAC used in this study differs from the one documented in van Zanten et al. (2010) in two main aspects: Firstly, the implementation of a function considering co-deposition of SO₂ and NH₃ (Wichink
 210 Kruit et al., 2017) in the non-stomatal pathway and secondly, the usage of a monthly moving NH₃ average concentration for determining the stomatal compensation point (Wichink Kruit et al., 2017).

2.2.2 Modeling of ΣN_r deposition (LOTOS-EUROS)

LOTOS-EUROS (Manders et al., 2017) simulations were performed for the entire measurement period. For this purpose, a large-scale simulation was setup for Europe in which a second domain covering northwestern Europe at 7x7 km² was nested.
 215 The simulations were forced with weather data from the ~~European Centre for Medium range Weather Forecast (ECMWF)~~ and the CORINE-2012 land-use classification. For the European background simulation, the CAMS-REG European emission inventory (Kuenen et al., 2021) was used. For the inner domain the emission data for Germany were replaced by the national emission inventory. ~~For Germany, the gridded emissions were obtained from the GrETa system (GRETA – Gridding Emission Tool for ArcGIS v1.1; Schneider et al., 2016). Modeled concentrations were written out for a reference height of 2.5 m. The~~
 220 ~~land use specific and total dry deposition were calculated by LOTOS-EUROS on hourly basis for NH₃, NO, NO₂, HNO₃, NO₃⁻, and NH₄⁺. Dry deposition of particles was calculated according to Zhang et al. (2001) (see Manders-Groot et al. (2016, Sect. 5.2)).~~ On hourly basis, the land-use specific total dry deposition was calculated in LOTOS-EUROS by applying DEPAC for NH₃, NO, NO₂, and HNO₃. Dry deposition of pNO₃⁻ and pNH₄⁺ was calculated according to Zhang et al. (2001) (see Manders-Groot et al. (2016, Sect. 5.2)). In the model, the dry deposition velocity and flux are calculated for the mid-layer height of the
 225 first model layer, which has a depth of ca. 20 m. By assuming a constant flux and using the stability parameters, the concentrations can be estimated for the canopy top and the typical observation height (2.5 m above roughness length (z_0)) in air quality networks. The Corine Land Cover 2012 classification of the grid cell, in which the measurement site was located, was divided into 46.0 % seminatural vegetation, 37.2 % coniferous forest, 15.9 % deciduous forest, 0.7 % water bodies, and 0.2 % grassland. However, the actual structure of the forest stand showed 81.1 % coniferous forest and 18.9 % deciduous
 230 forest within the footprint of the flux measurements during the measurement campaign. Due to differences in the distribution of vegetation types in the footprint, results from LOTOS-EUROS were calculated with the site-specific weighting of land-use classes of the flux tower's footprint. The low contribution of coniferous forest and deciduous forest within the grid cell may be related to the evaluation of older aerial photographs showing larger areas of deadwood. Finally, the dry deposition of ΣN_r was calculated as the sum of the individual N_r fluxes. A detailed documentation of LOTOS-EUROS is given in Manders-Groot
 235 et al. (2016) and Manders et al. (2017).

2.2.3 Site-based modeling of ΣN_r deposition (DEPAC-1D)

DEPAC-1D is a stand-alone version of LOTOS-EUROS' dry deposition module DEPAC using a FORTRAN90 wrapper program to accept arbitrary input datasets. DEPAC-1D used micrometeorological variables and parameters measured at the site to estimate R_c and the compensation point of NH₃. The atmospheric resistances – R_a and R_b – and the fluxes of NH₃, NO,
 240 NO₂, HNO₃, pNO₃⁻, and pNH₄⁺ were calculated outside DEPAC following Garland (1977) and Jensen and Hummelshøj (1995,

1997) with stability corrections after Webb (1970) and Paulson (1970). The deposition of particles was calculated following Zhang et al. (2001) (see also Manders-Groot et al. (2016, Sect. 5.2)) and therewith equal to LOTOS-EUROS. For the fine fraction of pNO_3^- and pNH_4^+ , a mass median diameter of $0.7 \mu\text{m}$ was used. For the coarse fraction of pNO_3^- , $8 \mu\text{m}$ was taken (Manders-Groot et al. (2016, Sect. 5.2)). Note that particle deposition is strictly speaking not part of the DEPAC module and was modeled with a separate program implementing the particle deposition scheme used within LOTOS-EUROS.

~~For estimating fluxes with DEPAC 1D, concentration measurements on monthly and half hourly basis were used. NH_3 fluxes were mostly based on half hourly concentration measurements of the NH_3 QCL. Half-hourly gaps in the NH_3 QCL concentration time series were assigned-filled with their monthly integrated concentration value obtained from DELTA samplers. If these measurements were not available, missing values were replaced by monthly integrated results from passive sampler measurements of NH_3 . During winter, the uncertainty introduced by this gap-filling approach seems to be low as suggested by Schrader et al. (2018). We did not superimpose gap-filled concentration values with a diurnal pattern or used monthly averages of half-hours to fill gaps in concentration time series, since instationaries abrupt changes in the NH_3 concentration pattern, i.e. periods of low auto-correlation could not be reproduced by a synthetic diurnal cycle or monthly averages of half-hourly values. Fluxes of HNO_3 , NO_3^- , and NH_4^+ solely based on monthly DELTA measurements. Gaps in time series of these compounds and SO_2 were replaced by monthly averages from adjacent years. NO and NO_2 fluxes were based on half-hourly concentration measurements routinely taken at 50 m. The difference in measuring height was considered in the calculation of R_a . SO_2 and NH_3 concentrations from gap-filled DELTA time series were used to determine compensation points and additional deposition corrections, similar to the use of monthly averages when using DEPAC within LOTOS-EUROS.~~

~~All micrometeorological parameters were available at half hourly resolution. Since measurements of T temperature and relative humidity data were not available at the measurement height of the EC system, we took corresponded to the average of measurements from 20 m and 40 m height above ground. Since These profile measurements of temperature and relative humidity started in April 2016 (Wintjen et al., 2022), and thus measurements at 50 m were used until end of March 2016. Pressure and global radiation measurements were taken at 50 m, too. Indicators of stability and turbulence such as the Obukov length and friction velocity were obtained from momentum flux measurements of the sonic anemometer. For modeling R_a , the solar zenith angle, which is calculated by using celestial mechanic equations, the roughness length (z_0), and d are needed. We set z_0 to 2.0 m and d to 12.933 m for coniferous forest and to 11.60 m for deciduous forest, corresponding to LOTOS-EUROS defaults for these land-use classes. Leaf area index (LAI) was modeled as described by van Zanten et al. (2010). The LAI determined from the site-specific land-use class weighting ranged between 4.1 and 4.8 due to leaf growth and shedding.~~

The calculation of the dry deposition was made for NH_3 , NO , NO_2 , HNO_3 , pNO_3^- , and pNH_4^+ with the mentioned input data on half-hourly basis. Results from DEPAC-1D were weighted with the site-specific land-use distribution within the flux measurement's footprint (81.1 % coniferous forest and 18.9 % deciduous forest). ~~We compared them to dry deposition fluxes of LOTOS EUROS as well as the measured ΣN_x fluxes estimated with the EC method from TRANC measurements (Wintjen, et al. 2022). In order to compare the results from modeling to TRANC measurements, we filled gaps in the TRANC flux data given by Wintjen et al. (2022) with results from DEPAC 1D. Those gaps were related to insufficient turbulence mostly occurring during nighttime, performance issues of the instruments, etc. Gaps in DEPAC 1D were mostly related to power outages causing gaps in micrometeorological data and issues in the measurements of N_x compounds. Respective half hourly values in the flux time series of each gas (approx. 3.4% for NH_3 , HNO_3 , NH_4^+ , and NO_2^- and 9.3% for NO and NO_2) were filled with results from LOTOS EUROS. We further made a combination of Mean Diurnal Variation (MDV) approach (Falge et al., 2001) and DEPAC 1D. Analogous to Wintjen et al. (2022), MDV was applied to short term gaps (less than 3 days), but instead of using monthly diurnal averages of specific half hours to replace missing values in long term gaps we used DEPAC 1D. The~~

285 window for filling a gap with MDV was set to ± 5 days, gaps spanning time frames of more than 3 days were treated as long-term. Both approaches, DEPAC-1D alone and the combination of DEPAC-1D and MDV, were able to fill all gaps in flux time series. Uncertainties of the gap-filled fluxes determined by MDV were calculated as the standard error of the mean. Cumulative uncertainties of TRANC fluxes solely based on the uncertainty of the gap filling and were calculated according to Eq. (3) of Wintjen et al. (2022). The error calculation scheme proposed by Brümmer et al. (2022) (Eq. (1)) was applied to fluxes filled with DEPAC-1D. Flux uncertainty of those half hours was given as

$$F_{\text{unc,DEPAC-1D}} = \frac{\tilde{X}}{F_{\text{DEPAC-1D}}}; \text{ with } \tilde{X} = \frac{F_{\text{unc,meas}}}{F_{\text{meas}}} \quad (5)$$

290 where \tilde{X} represents the median of the ratio of the uncertainty of the measured fluxes ($F_{\text{unc,meas}}$) to their corresponding flux values (F_{meas}). The uncertainty of the measured fluxes was given by Finkelstein and Sims (2001). Systematic uncertainties were not accounted in the error calculation. A discussion on systematic uncertainties is given in Wintjen et al. (2022).

295 2.3 Measuring nitrogen outflow from the canopy using the Canopy Budget ~~technique~~ Technique (CBT)

The canopy budget technique (CBT) is the most common method for estimating ~~total and dry nitrogen deposition in ecological field research based on inorganic nitrogen fluxes (NO_3^- , NH_4^+)~~ only total (wet+dry) atmospheric deposition of dissolved inorganic nitrogen (DIN_t) based on wet inorganic nitrogen fluxes of NO_3^- and NH_4^+ -ions estimated from open-site precipitation (bulk deposition) and throughfall of NO_3^- and NH_4^+ -ions measurements (see Staelens et al., 2008, Table 1).
 300 ~~Total deposition of dissolved inorganic nitrogen (DIN_t)~~ was estimated on ~~yearly~~ monthly basis after the CBT approach of Draaijers and Erisman (1995) and de Vries et al. (2003). ~~whose~~ The results from the two methods differed only marginally and were therefore averaged. The biological conversion of deposited inorganic nitrogen into dissolved organic nitrogen (DON) in the ~~canopy~~, phyllosphere (bacteria, yeasts, and fungi) or the dry deposition of atmospheric DON onto the canopy or the exudation of DON from plant tissues ~~which~~ is not addressed in CBT. Here, it was estimated by the difference of DON
 305 fluxes between throughfall and bulk deposition, and henceforth called (ΔDON). Adding ΔDON to throughfall DIN_t or to DIN_t reveals a frame of lower and upper estimates of total (wet+dry) nitrogen deposition (N_t) and, by subtracting DIN_t deposition at an open land site from these N_t , of lower and upper estimates of dry deposition (Beudert and Breit, 2014).

3 Results

310 3.1 Comparison of modeled and measured concentrations

3.1.1 High resolution concentration measurements of NH_3 , NO_x , and ΣN_t

Figure 1 shows the comparison of measured half-hourly NH_3 , NO_x , and ΣN_t concentrations (cf. Wintjen et al., 2022) to their modeled concentrations of LOTOS-EUROS represented as monthly box-whisker plots. From high-resolution concentration
 315 measurements, we found average concentrations and standard deviations of 1.0 ± 0.6 , 1.4 ± 1.2 , and $3.1 \pm 1.7 \mu\text{g N m}^{-3}$ for NH_3 , NO_x , and ΣN_t for the entire campaign, respectively. Corresponding averages of LOTOS-EUROS of NH_3 and ΣN_t were higher by 0.8 and $1.9 \mu\text{g N m}^{-3}$, whereas NO_x was slightly underestimated. Substantial mismatches in standard deviations of NH_3 and ΣN_t indicate that the variability in concentrations of NH_3 and ΣN_t was overestimated by LOTOS-EUROS. In case of NH_3 , largest discrepancies were observed for spring and partially for autumn. NO_x concentrations were systematically
 320 underestimated by LOTOS-EUROS in summer. During winter, difference between measured and modeled NO_x concentrations was lower than during summer time. ~~Figure 1 shows the modeled concentrations of LOTOS-EUROS for each N_t compound~~

and their sum in comparison to the TRANC measurements. Looking at concentrations and patterns of each of the individually modeled compounds, reveals that NH_3 had the highest concentrations, in particular in spring and partially in autumn with values close to zero in winter. On average, LOTOS-EUROS predicted an average NH_3 concentration of $1.8 \mu\text{g N m}^{-3}$. During spring, modeled concentrations exceeded $10 \mu\text{g N m}^{-3}$. Such high concentration levels were not reached by the other N_x compounds. In winter, NO_2 concentrations reached up to $5 \mu\text{g N m}^{-3}$, whereas concentrations were negligibly small in summer. The concentrations of NO and HNO_3 were close to zero during the entire measurement campaign. Only during summer HNO_3 showed slight variations. Average concentrations of NO_2^- and NH_4^+ were similar to NO_2 . Particle concentrations were lowest in summer and reached values up to $5 \mu\text{g N m}^{-3}$ in spring. The comparison of measured and modeled ΣN_x revealed significant discrepancies in concentration values. Except for the summer, modeled half-hourly concentrations of ΣN_x were two to three times higher than the measured values. The slight seasonal differences in measured ΣN_x concentrations could not be reproduced by LOTOS-EUROS. Average ΣN_x concentration modeled with LOTOS-EUROS was $5.0 \mu\text{g N m}^{-3}$, whereas the average measured concentration with the TRANC was $3.1 \mu\text{g N m}^{-3}$. The largest discrepancy being largest during spring clearly correlates with the modeled ammonia- NH_3 concentrations.

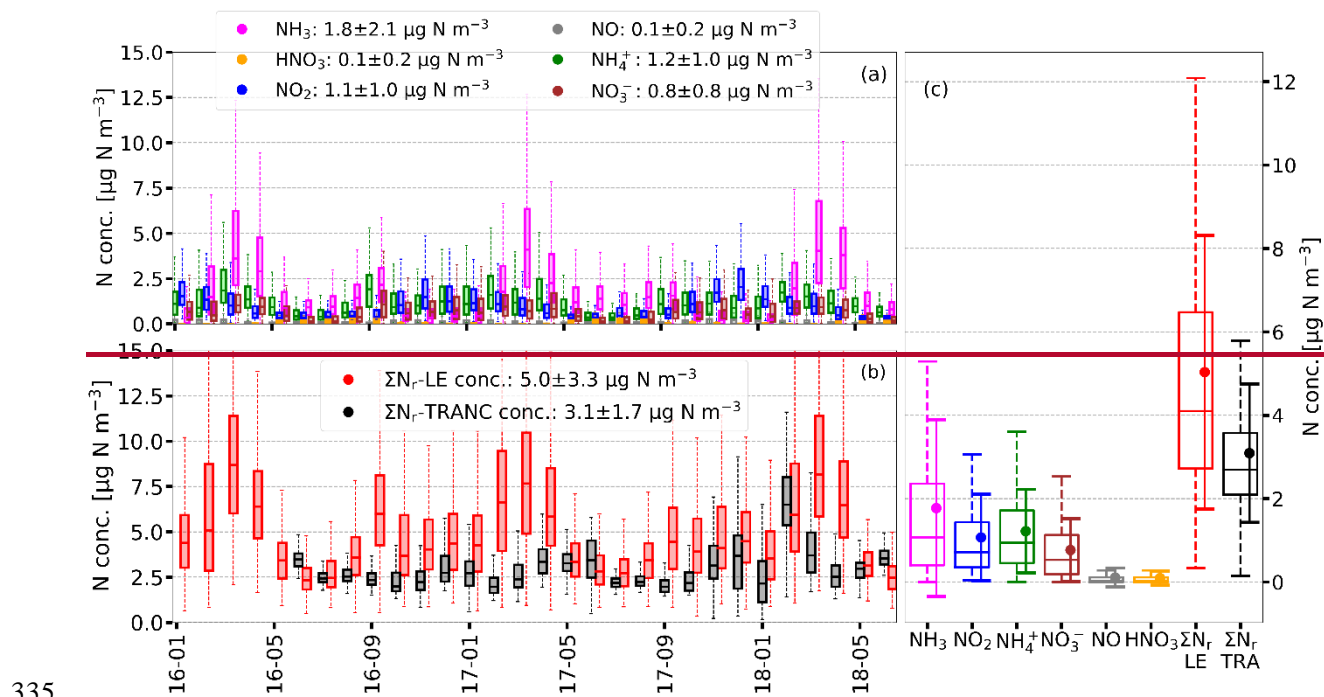
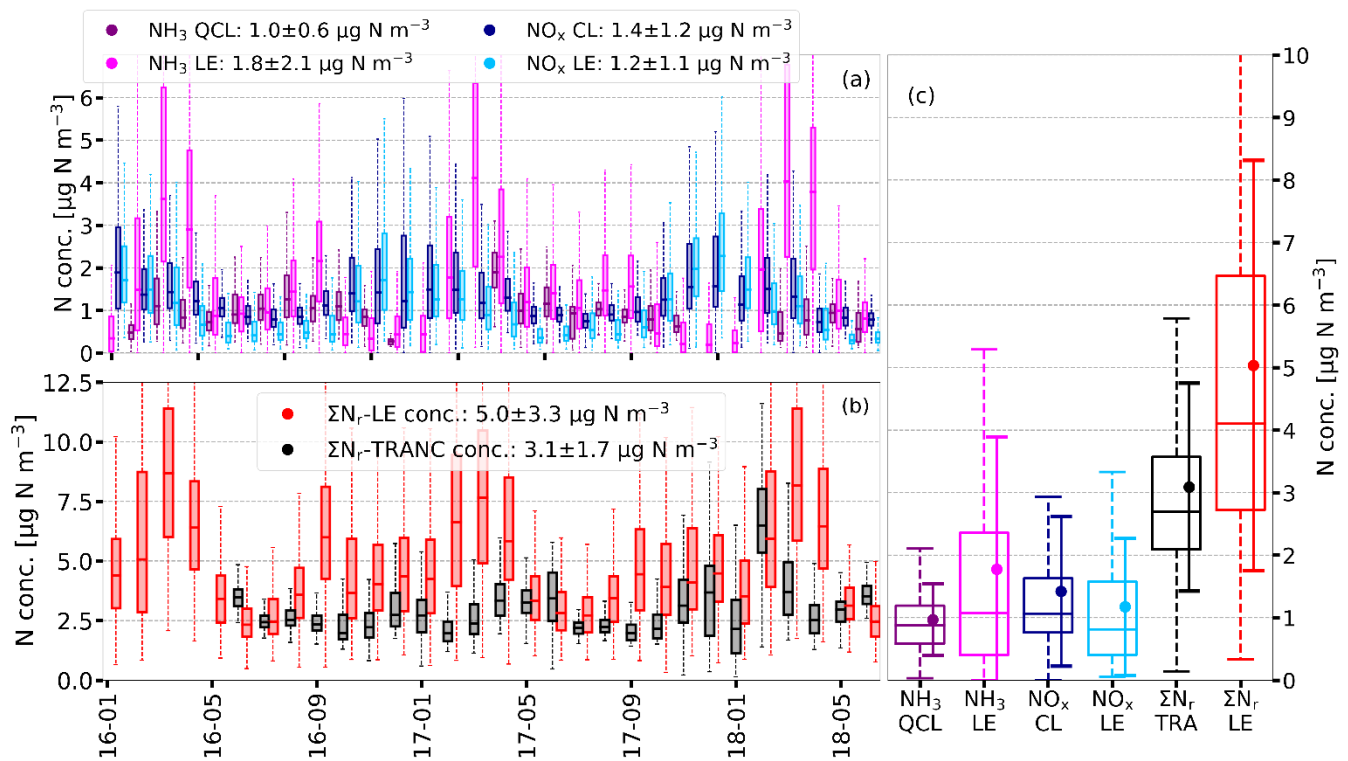


Figure 1. Concentrations of NH_3 (fuchsia), NO_2 (blue), NO (grey), HNO_3 (orange), NH_4^+ (green), NO_3^- (brown), and their corresponding sum (red) predicted by LOTOS-EUROS (LE) compared to ΣN_x (black) obtained from TRANC measurements represented as box and whisker plots (box frame = 25% to 75% interquartile range (IQR), bold line = median, whisker = $1.5 \times \text{IQR}$) on monthly basis ((a) and (b)) and for the entire duration of the campaign (January 2016 to end of June 2018) (c) in $\mu\text{g N m}^{-3}$. In the legends, averages and standard deviations referring to the entire campaign for ΣN_x and its individual compounds are shown.



345

Figure 1. Half-hourly concentrations of NH_3 , NO_x , and ΣN_r obtained from quantum-cascade-laser (QCL), chemiluminescence (CL), and TRANC (TRA) measurements compared to LOTOS-EUROS (LE) results displayed as box-whisker plots (box frame = 25 % to 75 % interquartile range (IQR), bold line = median, whisker = $1.5 \cdot \text{IQR}$) on monthly basis ((a) and (b)) and for the entire duration of the campaign (January 2016 to end of June 2018) (c) in $\mu\text{g N m}^{-3}$. Darker colors represent the results from measurements, brighter colors from LOTOS-EUROS. In the legends, averages and standard deviations referring to the entire campaign for NH_3 , NO_x , and ΣN_r are shown.

3.1.2 Passive samplers and DELTA measurements

350

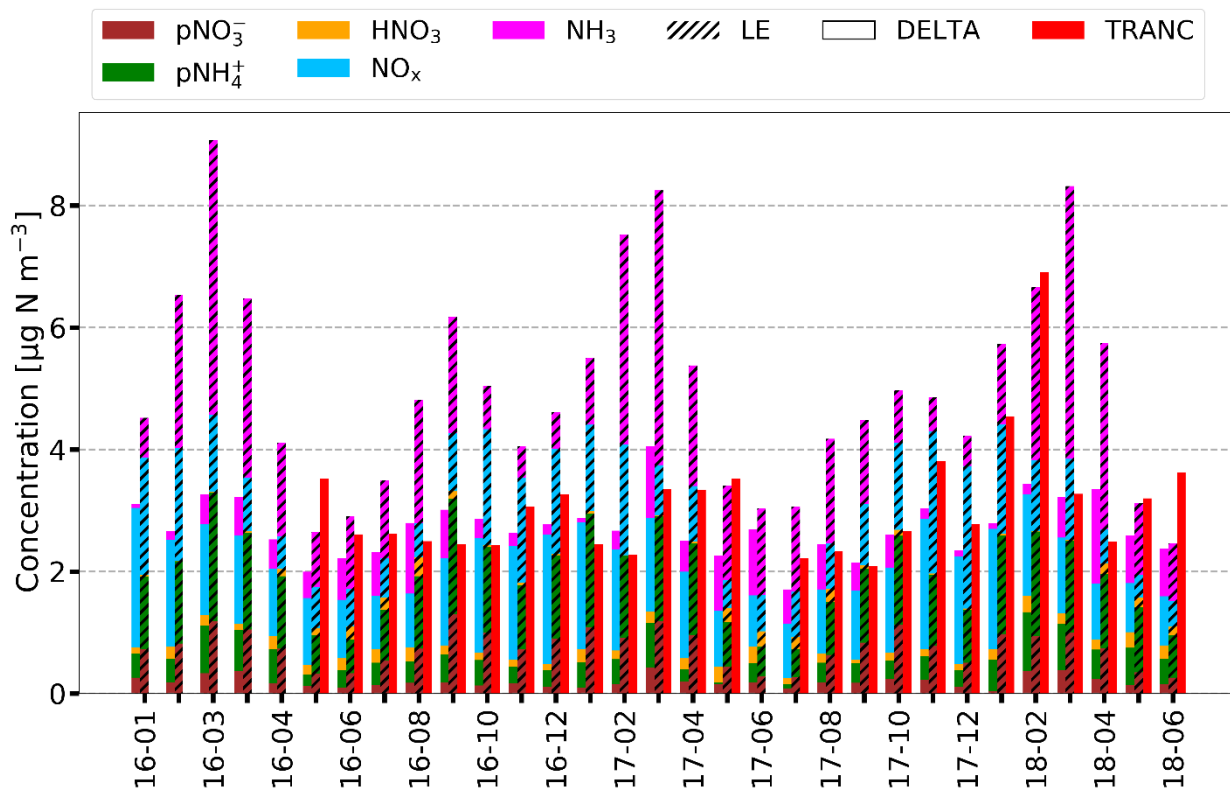
The large modeled NH_3 concentrations by LOTOS-EUROS could also not be verified by the observed levels of the passive samplers, and the DELTA system, and the QCL. Figure S1 shows a comparison of the applied NH_3 measurement techniques with NH_3 concentrations predicted by LOTOS-EUROS. A two- to threefold overestimation of NH_3 concentrations by LOTOS-EUROS is visible. In addition, the modeled seasonal pattern was also not in agreement with the results from wet chemical samplers. measurements, for example, the increase in NH_3 during autumn was not observed by the instruments.

355

A comparison of the individual measured N_r compounds by DELTA to LOTOS-EUROS is displayed in Fig. 2. Considering the entire campaign, we measured average concentrations of 0.55 , 0.17 , 0.42 , and 0.19 $\mu\text{g N m}^{-3}$ for NH_3 , HNO_3 , pNH_4^+ , and pNO_3^- , respectively. For the same exposure periods, the concentration averages of LOTOS-EUROS for NH_3 , HNO_3 , pNH_4^+ , and pNO_3^- were 1.8 , 0.1 , 1.2 , and 0.8 $\mu\text{g N m}^{-3}$, respectively. Differences considering the entire campaign duration are shown in Fig. S2. Like NH_3 , particulate nitrogen compounds concentrations were also higher in the LOTOS-EUROS simulations. Predicted seasonality for pNH_4^+ and pNO_3^- could only partially be verified by DELTA measurements. For HNO_3 , concentrations were in close agreement. The discrepancy in the seasonal pattern of NH_3 is obvious. The distinct peaks occurring in February, March, April, September, and October were not found by DELTA. In total, ΣN_r values of DELTA and TRANC showed a reasonable agreement and ΣN_r concentrations showed only small seasonal differences whereas LOTOS-EUROS overestimated ΣN_r of the TRANC by ca. 2 $\mu\text{g N m}^{-3}$ (Fig. S2).

365

The high ΣN_r concentrations of LOTOS-EUROS were mainly related to NH_3 . In addition, NO_2^- and NH_4^+ were not in agreement with values determined by DELTA. Considering the entire campaign, median differences to DELTA were 0.57 , 0.77 , and 0.87 $\mu\text{g N m}^{-3}$ for NH_3 , NO_2^- , and NH_4^+ , respectively (see Fig. S2). HNO_3 concentrations agreed well (0.08 $\mu\text{g N m}^{-3}$), and NO_x was slightly lower in the LOTOS-EUROS simulations (0.32 $\mu\text{g N m}^{-3}$) (Fig. S2).



370

375

380

385

390

Figure 2. Monthly stacked concentration of LOTOS-EUROS (LE) (hatched), TRANC (grey red), DELTA, and NO_x in µg N m⁻³ for the entire measurement campaign. Gaps in the NH₃ timeseries caused by a low pump flow of the denuder pump were filled with passive sampler values from 30 m. This procedure was done for December 2016 and 2017, March 2018, and April 2018. Remaining gaps in the time series of HNO₃, pNH₄⁺, and pNO₃⁻ were replaced by monthly averages estimated from other years if available. In case of NH₃, the procedure was applied to January 2017. For the other compounds, the gap-filling was done for December 2017, March 2018, and April 2018. Results from LOTOS-EUROS, TRANC, and NO_x measurements were averaged to the exposure periods of the DELTA samplers. In the small panel, the difference in the monthly ΣN_r concentrations of TRANC and LOTOS-EUROS is shown represented as box-whisker plot (box frame = 25 % to 75 % interquartile range (IQR), bold line = median, whisker = 1.5*IQR) (red) and average with error bars indicating the standard deviation (black) for the entire measurement campaign.

According to Wintjen et al. (2022), NO_x was the Since NH₃ contributed most to ΣN_r in LOTOS-EUROS, seasonal contributions of the N_r compounds were different to results determined from DELTA and NO_x measurements. Wintjen et al. (2022) determined NO_x as predominant compound in the ΣN_r concentrations. For the entire campaign, NO_x contributed 51.4 % and NH₃ 20.0 % to measured ΣN_r, whereas LOTOS-EUROS states-predicted the NH₃ as the most important compound (~35.7 %) contributing to ΣN_r, followed by pNH₄⁺ (~24.3 %), NO_x (~22.8 %), pNO₃⁻ (~15.2 %), and HNO₃ (~1.9 %) as shown by Fig. S3. Furthermore, LOTOS-EUROS showed deviations from measurements in seasonal contributions. By comparing Fig. S3 and Fig. 2, we examined that LOTOS-EUROS and DELTA found seasonal changes for NH₃ with the highest contribution in spring and lowest in winter. However, During winter, the contribution of NH₃ to ΣN_r was surprisingly high (28.6 %) compared to the observations (4.9 %) during winter. As expected from Fig. 2, HNO₃ contributions were comparable and on a low level between LOTOS-EUROS and DELTA. On average, pParticle contribution was higher in the model. Contributions of pNO₃⁻ and pNH₄⁺ were highest during spring according to measurements but lowest in LOTOS-EUROS in that season. Apart from springtime, seasonal contributions of pNO₃⁻ and pNH₄⁺ were higher by 6.6 to 14.4% in LOTOS-EUROS, and their contributions and concentrations were invariant to seasonal changes except for spring.

3.2 Modeled N_r -deposition velocities and fluxes of DEPAC-1D Comparison of modeled and measured deposition velocities

395

The comparison of the deposition velocities and fluxes for each N_r compound modeled by DEPAC-1D is shown in Fig. S4 and S5 displayed as monthly box- and whisker plots, respectively. For the data description, medians were preferred to reduce the influence of outliers on reported deposition velocities and fluxes.

In case of HNO_3 , a median v_d of 1.56 cm s^{-1} was determined by DEPAC-1D. During the entire campaign, IQR and positions of the whiskers showed less interseasonal variations with largest values of 4.27 cm s^{-1} . From May to September, the flux median was $3.35 \text{ ng N m}^{-2} \text{ s}^{-1}$ whereas $2.04 \text{ ng N m}^{-2} \text{ s}^{-1}$ was determined for the other months. Largest fluxes were found for May and June with values close to $10.0 \text{ ng N m}^{-2} \text{ s}^{-1}$ caused by slightly higher concentrations compared to the rest of the year. Deposition velocities of NO_2 were close to zero in winter. From April to October, monthly median deposition velocities ranged between 0.07 and 0.35 cm s^{-1} with largest values ($1.5 \cdot \text{IQR}$; see Fig. S4) close to 1.0 cm s^{-1} . The seasonal pattern in v_d is transferable to the predicted fluxes. Fluxes were enlarged from April to October, but flux medians showed hardly any monthly variations, and flux median was at $1.57 \text{ ng N m}^{-2} \text{ s}^{-1}$. Similar to HNO_3 , largest fluxes ($1.5 \cdot \text{IQR}$; see Fig. S5) reached up to $10.0 \text{ ng N m}^{-2} \text{ s}^{-1}$. Modeled deposition velocities of and fluxes of NO were the lowest in DEPAC-1D and negligible compared to the other compounds

Only during winter, monthly median deposition velocities of NH_3 were close to zero. From March to August, deposition velocities were larger, and monthly medians ranged between 0.55 and 2.17 cm s^{-1} but extensions of the IQR and whiskers in the boxplots were similar (Fig. S4). Overall, the median NH_3 deposition was $7.87 \text{ ng N m}^{-2} \text{ s}^{-1}$ for DEPAC-1D. From the seasonal point of view, hardly any deposition was predicted for winter, and a median deposition of $10.52 \text{ ng N m}^{-2} \text{ s}^{-1}$ was found during spring.

Monthly median deposition velocities of NO_2^- and NH_4^+ followed the same temporal pattern with lower values lowest in summer and higher in winter. During summer, monthly median deposition velocities were close to zero. Median v_d was 0.01 and 0.05 cm s^{-1} for NO_2^- and NH_4^+ during winter, respectively. Only in February 2018, whiskers of DEPAC-1D extended up to 0.37 and 1.27 cm s^{-1} for NO_2^- and NH_4^+ , respectively. For the entire campaign, DEPAC-1D monthly flux medians of NO_2^- and NH_4^+ were lower than 0.05 and $0.60 \text{ ng N m}^{-2} \text{ s}^{-1}$. In February 2018, whiskers for DEPAC-1D extended to 11.0 and $1.0 \text{ ng N m}^{-2} \text{ s}^{-1}$ for NH_4^+ and NO_2^- , respectively (see Fig. S5).

3.2.1 Comparison of modeled and measured deposition velocities for each N_r compound

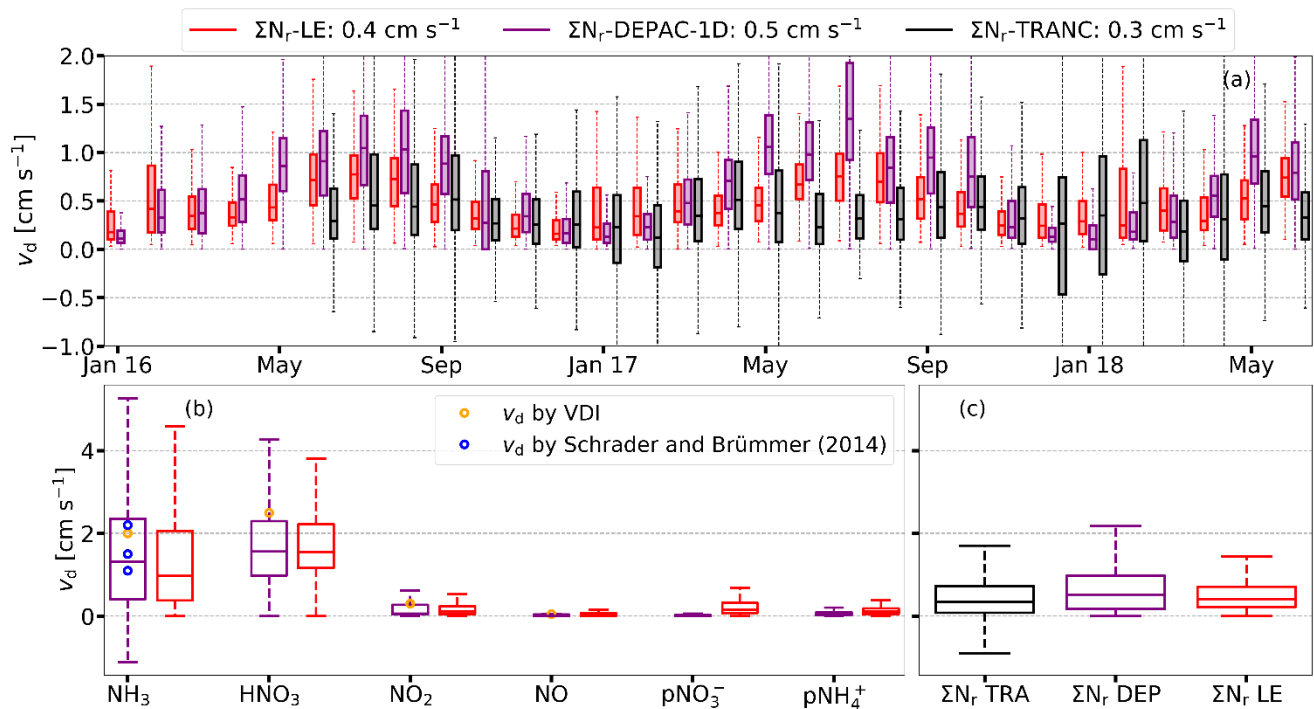
420

NH_3 deposition velocities of LOTOS-EUROS and DEPAC-1D exhibited similar values in winter, but disagreements were found in summer and autumn. In summer, DEPAC-1D determined systematically larger median deposition velocities, whereas LOTOS-EUROS predicted a large variability in NH_3 deposition velocities during autumn, which was not supported by DEPAC-1D. For NO_2 , deposition velocities of LOTOS-EUROS and DEPAC-1D agreed well in their temporal pattern and the median deposition velocities, but the variability in DEPAC-1D deposition velocities was slightly higher during summer. In both model applications, NO deposition velocities were practically zero (medians always $< 0.06 \text{ cm s}^{-1}$). For pNH_4^+ , deposition velocities of DEPAC-1D and LOTOS-EUROS agreed well with median deposition velocities close to zero, but a large disagreement was found during winter. Deposition velocities of pNO_3^- were close to zero during the entire campaign in DEPAC-1D, but LOTOS-EUROS showed a large scattering of v_d in the winter months. For HNO_3 , a discrepancy in v_d was also found during winter, and, similar to NH_3 , deposition velocities of DEPAC-1D were generally larger from May to September. The comparison of the deposition velocities for each N_r compound modeled by DEPAC-1D and LOTOS-EUROS is shown in Fig. S4.

430

3.2.2 Comparison of modeled and measured ΣN_r deposition velocities

435 A comparison of the modeled and measured v_d for the ΣN_r flux is provided in Fig. 3. The modeled total nitrogen dry deposition velocities were obtained by dividing the modeled dry deposition flux for all compounds by the modeled total nitrogen concentrations in ambient air. Subtracting median v_d of TRANC from LOTOS-EUROS results, Differences between the median modeled and measured v_d typically ranged between -0.3 and 1.0 cm s^{-1} . Especially during the summer months, an overestimation of the modeled values was observed for the v_d by DEPAC-1D results was observed with respect to TRANC measurements. During those months, median v_d of DEPAC-1D was ca. 2 to 3 times higher than their measured entities. LOTOS-EUROS v_d of the ΣN_r flux were generally lower than DEPAC-1D but still larger than found in the measurements within that period. During the winter months, DEPAC-1D ΣN_r showed lowest median values and variability, whereas deposition velocities of TRANC and LOTOS-EUROS were comparable caused by influence of pNO_3^- and pNH_4^+ on LOTOS-EUROS v_d predictions. The modeled median values and diurnal cycles for winter months were quite comparable to the measured values.

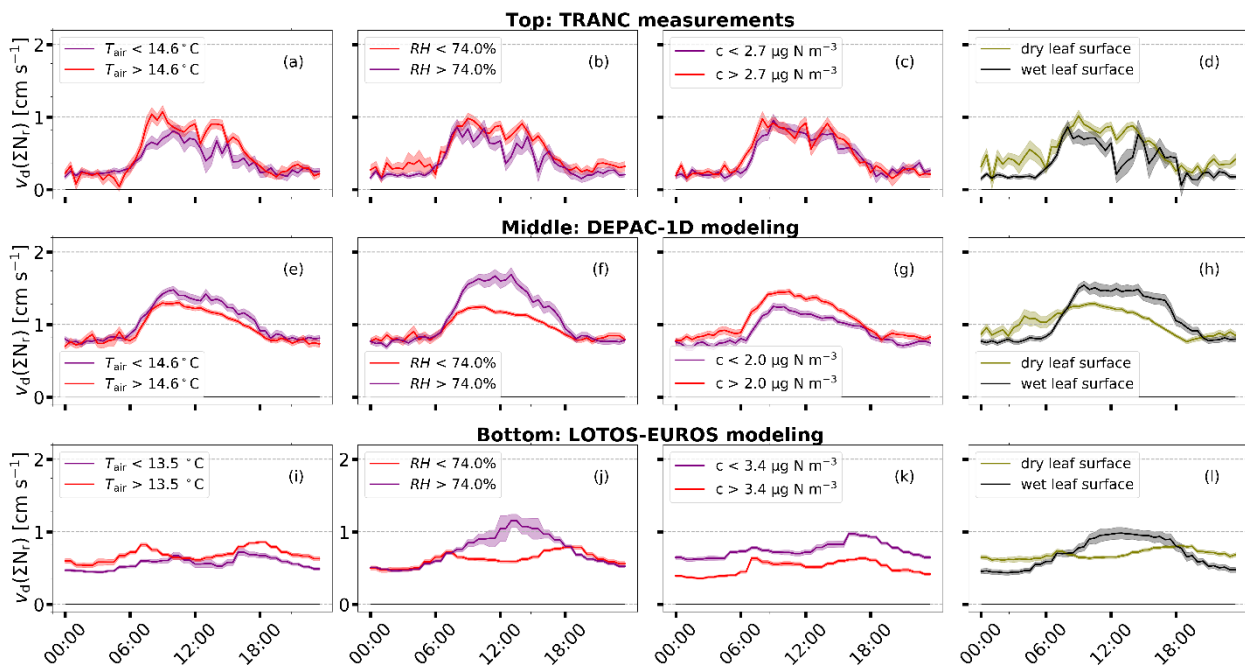


450 **Figure 3.** Monthly v_d of ΣN_r determined from TRANC (purple/black) measurements, DEPAC-1D (black/purple), and LOTOS-EUROS (red) with the corrected land-use weighting in cm s^{-1} represented as box-and-whisker plots in the upper panel (a). In the corresponding legend median v_d related to the entire campaign are given. In the lower panels ((b) and (c)), box-and-whisker plots of v_d for each N_r compound and ΣN_r are shown based on the entire campaign (TRA=TRANC, DEP=DEPAC-1D, LE= LOTOS-EUROS). Blue circles are referring to NH_3 deposition velocities reported by Schrader and Brümmer (2014) for deciduous forest, mixed forest, and spruce forest (from low to high), orange circles show deposition velocities proposed by VDI (2006).

455 As the DEPAC-1D was fed with measured concentration data, the comparison for the modeled ΣN_r fluxes shows a large degree of similarity to the results for the deposition velocity, see Fig. 6. The ΣN_r exchange of DEPAC-1D is close to zero during the entire winter, and thus the difference to measured deposition was lowest during that time. During summer, a systematic overestimation of DEPAC-1D compared to measured fluxes was observed. Inspection of the diurnal cycles of ΣN_r deposition velocities for May to September in the year 2017 (Fig. S7) shows that both, the DEPAC-1D and measured data, exhibit a clear diurnal pattern with lowest deposition during the night and highest values around noon. However, in those periods where the measured data are close to zero during the night, the modeled fluxes show considerable nighttime exchange fluxes. The latter may be due to the assumption of constant HNO_3 concentrations as input to DEPAC-1D, whereas in reality the concentrations

are low at night and maximize during the day. Note that improving this issue would result in an even larger overestimation of the flux during daytime.

465 To further examine the reasons behind these discrepancies, we show the diurnal cycles of v_d after classifying the ΣN_r deposition velocities for half-hours without precipitation during May-September in two groups being below or above the median temperature ($T_{air}=14.6^\circ\text{C}$), relative humidity ($RH=74.0\%$), and total ΣN_r concentration ($c(\Sigma N_r)=2.7\ \mu\text{g N m}^{-3}$). In addition, we separated dry and wet leaf surfaces following the calculation scheme by Wintjen et al. (2022). Leaf surface wetness was measured at the site with sensors attached to a spruce and a beech tree. In order to classify the sensor as dry or wet, the half-hourly leaf wetness value was compared to a threshold value based on the calculation scheme given by Wintjen et al. (2022).
 470 The diurnal cycles illustrate the same diurnal biases as discussed above. Figure 4 shows that DEPAC-1D results indicate that lower temperatures, higher relative humidity, and wet leaf surfaces enhance the ΣN_r dry deposition velocity. This behavior was expected based on the models' parameterization, but it is in contradiction to the TRANC measurements. Especially, the differences for the relative humidity regimes are remarkable. Smaller differences are observed for the dependency on temperature and the ΣN_r concentration, although both have a stronger influence in the model than on their measured counterpart.
 475 counterpart.



480 **Figure 4.** Averaged diurnal cycles of ΣN_r v_d for low and high temperature, relative humidity, concentration during the time frame May to September. The top row refers to TRANC measurements ((a) to (d)), the middle bottom row refers to DEPAC-1D modeling ((e) to (h)), and the bottom row to LOTOS-EUROS simulations ((i) to (l)). Data was stratified after their median calculated for the entire period. Dry and wet leaf surfaces (Panel (d) and (l)) were identified following the calculation scheme of Wintjen et al. (2022). Shaded areas represent the standard error of the mean.

In case of LOTOS-EUROS, separating diurnal cycles of v_d led to similar observations made for DEPAC-1D regarding relative humidity and leaf surfaces. In addition, lower temperatures and concentration tend to increase v_d , which contradicts the results of DEPAC-1D. Generally, values of v_d are closer to TRANC deposition velocities, but the diurnal pattern differs from those of TRANC and DEPAC-1D showing maxima in the morning (~06:00 LT) and evening (~18:00 LT) and low values around noon except for high relative humidity and wet leaf surfaces.
 485 of DEPAC-1D. Generally, values of v_d are closer to TRANC deposition velocities, but the diurnal pattern differs from those of TRANC and DEPAC-1D showing maxima in the morning (~06:00 LT) and evening (~18:00 LT) and low values around noon except for high relative humidity and wet leaf surfaces.

3.3 Modeled N_r deposition velocities and fluxes of LOTOS-EUROS Comparison of modeled and measured fluxes

490 Inspection of the dry deposition velocity for HNO_2 as calculated by LOTOS-EUROS (Fig. S4) showed a striking feature with unrealistically high values modeled for November 2017 to February 2018. Monthly median deposition velocities of LOTOS-EUROS were higher than $1.90\ \text{cm s}^{-1}$ and values of more than $10\ \text{cm s}^{-1}$ were reached. As v_d depends mostly on the aerodynamic resistance, a maximum is expected during summer and normally present. The periods with high v_d in winter are characterized

by snow cover. An error in the stability parametrization was found and will be corrected for after this study. The high v_d values during snow cover were present for all components for which subsequent resistances are small as well, i.e. HNO_3 , NH_3 , and nitrogen aerosols. The impact is also visible in the total nitrogen flux estimates, although not for all compounds. For example, the HNO_3 flux in winter is near to zero as nitric acid is almost not present. Also, for NH_3 the impact is small. The main impact is through the deposition of NO_3^- and NH_4^+ particles, which we will later correct for.

The deposition velocities of NH_3 of LOTOS-EUROS showed a seasonal pattern comparable to DEPAC-1D but deviations in absolute values were found. From April to August, we determined monthly medians ranging from 0.43 to 1.76 cm s^{-1} . Except for autumn, deposition velocities covered a wider range compared to DEPAC-1D. During that season, large values of up to 10.0 cm s^{-1} were reached. Differences in v_d of NO_2 to DEPAC-1D were negligible. From April to October, monthly median deposition velocities of LOTOS-EUROS were between 0.11 and 0.30 cm s^{-1} and close to zero in winter. Analogous to DEPAC-1D, deposition of NO did not play a role in the LOTOS-EUROS modeling. Deposition velocities of aerosol NO_3^- and NH_4^+ exhibited the same seasonal pattern. We determined a median v_d of 0.11 cm s^{-1} for NH_4^+ and 0.15 cm s^{-1} for NO_3^- .

From October to April, deposition fluxes of HNO_3 were nearly zero in LOTOS-EUROS but enlarged from May to September with a flux median of -1.56 $\text{ng N m}^{-2} \text{s}^{-1}$ and maximum values close to 10.0 $\text{ng N m}^{-2} \text{s}^{-1}$ (Fig. S5). Still, LOTOS-EUROS fluxes were generally lower than DEPAC-1D as represented by their monthly flux medians.

In case of NH_3 , a median deposition of 10.44 $\text{ng N m}^{-2} \text{s}^{-1}$ was predicted by LOTOS-EUROS. Compared to DEPAC-1D, LOTOS-EUROS monthly flux medians differed from zero during winter and extreme values in the order of 15.0 $\text{ng N m}^{-2} \text{s}^{-1}$ were written out. Outside the snow covered period, large discrepancies were recorded in February, March, and April. Medians of LOTOS-EUROS were higher by about 7.30 $\text{ng N m}^{-2} \text{s}^{-1}$. During spring, 14.58 $\text{ng N m}^{-2} \text{s}^{-1}$ were modeled with LOTOS-EUROS as median deposition.

In the LOTOS-EUROS simulations, NO_2 fluxes were generally lower and seasonal differences were less pronounced compared to DEPAC-1D. From April to October, a median flux of 0.96 $\text{ng N m}^{-2} \text{s}^{-1}$ was determined whereas 0.78 $\text{ng N m}^{-2} \text{s}^{-1}$ was calculated during the rest of the year. During winter, median depositions of NO_3^- and NH_4^+ were 1.40 and 1.76 $\text{ng N m}^{-2} \text{s}^{-1}$, respectively, with values higher than 10.0 $\text{ng N m}^{-2} \text{s}^{-1}$. During the rest of the year, median depositions of NO_3^- and NH_4^+ were approximately 0.65 and 0.78 $\text{ng N m}^{-2} \text{s}^{-1}$, respectively. Overall, the modeled and measured total nitrogen dry deposition velocities of LOTOS-EUROS and TRANC showed a slightly better agreement compared to DEPAC-1D, but v_d of LOTOS-EUROS were still higher during summer and substantially high in winter due to the influence of NO_3^- and NH_4^+ (see Fig. 3). Generally, deviations to the results of v_d for the ΣN_r flux were related to the input data of LOTOS-EUROS. The disagreements to measured concentrations were elaborated in Sect. 3.1, especially for NH_3 , but also for nitrogen aerosols (see Fig. 2 and S2) leading to discrepancies to TRANC fluxes in spring and winter (Fig. 6).

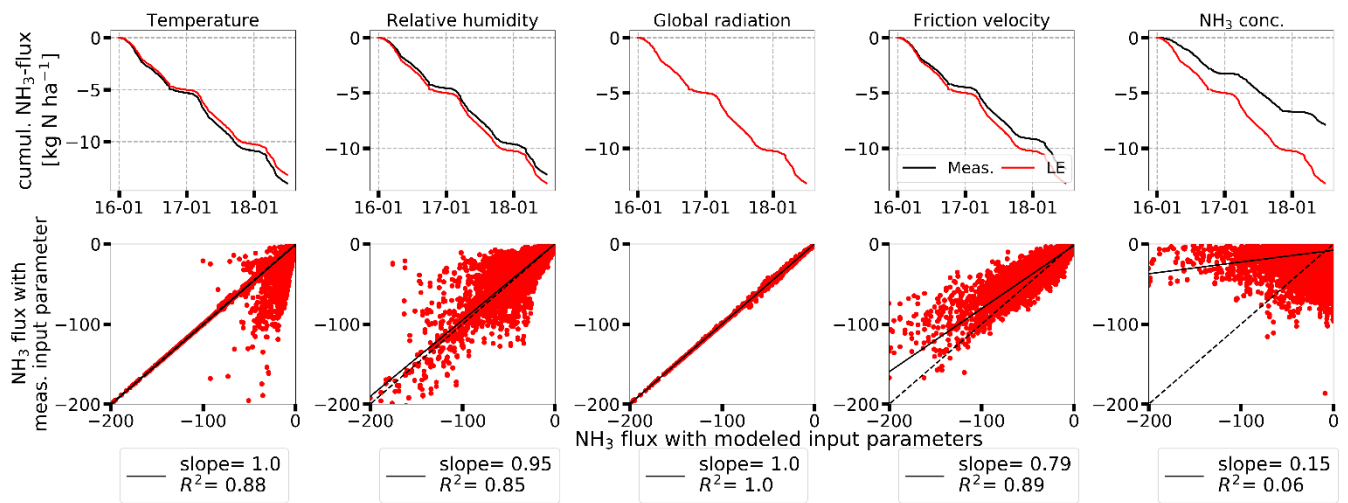
3.3.1 Influence of input concentrations and meteorology on modeled fluxes

The statements made for v_d can be transferred to the flux predictions. Differences to the observations made for v_d (Fig. S4) are related to the concentration input data. For example, due to overestimations of modeled NH_3 concentrations in spring and autumn, differences in fluxes were higher during the same time. Modeled NO_2 and HNO_3 concentrations of LOTOS-EUROS were lower than their measured values resulting in flux underestimations by LOTOS-EUROS for NO_2 and HNO_3 during summer. High modeled input concentrations of particulate nitrogen led to substantial deposition fluxes in the LOTOS-EUROS simulations. Following the model predictions, NH_3 fluxes had the largest contribution to the modeled ΣN_r flux with an average flux of -12.5 and -13.0 $\text{ng N m}^{-2} \text{s}^{-1}$ in the DEPAC-1D and LOTOS-EUROS applications, respectively, considering the entire campaign. Averaged fluxes of NO_2 and HNO_3 showed – although on a low level in absolute terms – higher deposition fluxes for DEPAC-1D, namely 2.0 and 1.3 $\text{ng N m}^{-2} \text{s}^{-1}$, respectively, compared to 1.2 and 0.3 $\text{ng N m}^{-2} \text{s}^{-1}$ in case of LOTOS-EUROS.

535 Substantial flux differences were found for particulate nitrogen. DEPAC-1D averaged fluxes were close to zero (0.9 and 0.1
ng N m⁻² s⁻¹ for pNH₄⁺ and pNO₃⁻, respectively), whereas LOTOS-EUROS showed substantial higher aerosol deposition with
averaged fluxes of 3.7 and 2.2 ng N m⁻² s⁻¹ for pNH₄⁺ and pNO₃⁻, respectively. The comparison of fluxes for each N_i compound
of LOTOS-EUROS and DEPAC-1D is shown in Figure S5.

540 Apart from concentrations being responsible for differences in modeled flux estimates, other parameters may have also been
contributed to the deviations. To further investigate the impacts of the input data used in the LOTOS-EUROS simulations, we
made a comparison of the measured and modeled input parameters used for the dry deposition modeling of NH₃ in LOTOS-
EUROS (Fig. S6). The agreement of temperature and global radiation in terms of their coefficient of determination R² was
good. We found ~~marginal~~ differences of approximately 1.5°C and -6.13 W m⁻² of modeled to measured values on average.
545 High R² values were determined for the entire campaign duration using half-hourly values, namely 0.97 for temperature and
0.78 for global radiation. A slight difference was found for relative humidity during the first half of 2016. However, modeled
values were higher by only 2.4 % on average, and the R² was still 0.67. In case of ~~u_z u_{*}~~, we found a systematic difference, and
the seasonal pattern did not agree well resulting in a lower R² of 0.43 compared to the other micrometeorological parameters.
~~Modeled values were higher by 0.09 m s⁻¹.~~ In particular from November 2017 to February 2018, the difference between
550 modeled and measured ~~u_z u_{*}~~ values was considerably large. ~~enlarged due to the snow cover effect. An increase in u_z reduces
turbulent resistances leading to large deposition velocities and fluxes for compounds like HNO₃, NO₃⁻, and NH₄⁺ which are
not or hardly affected by R_a.~~

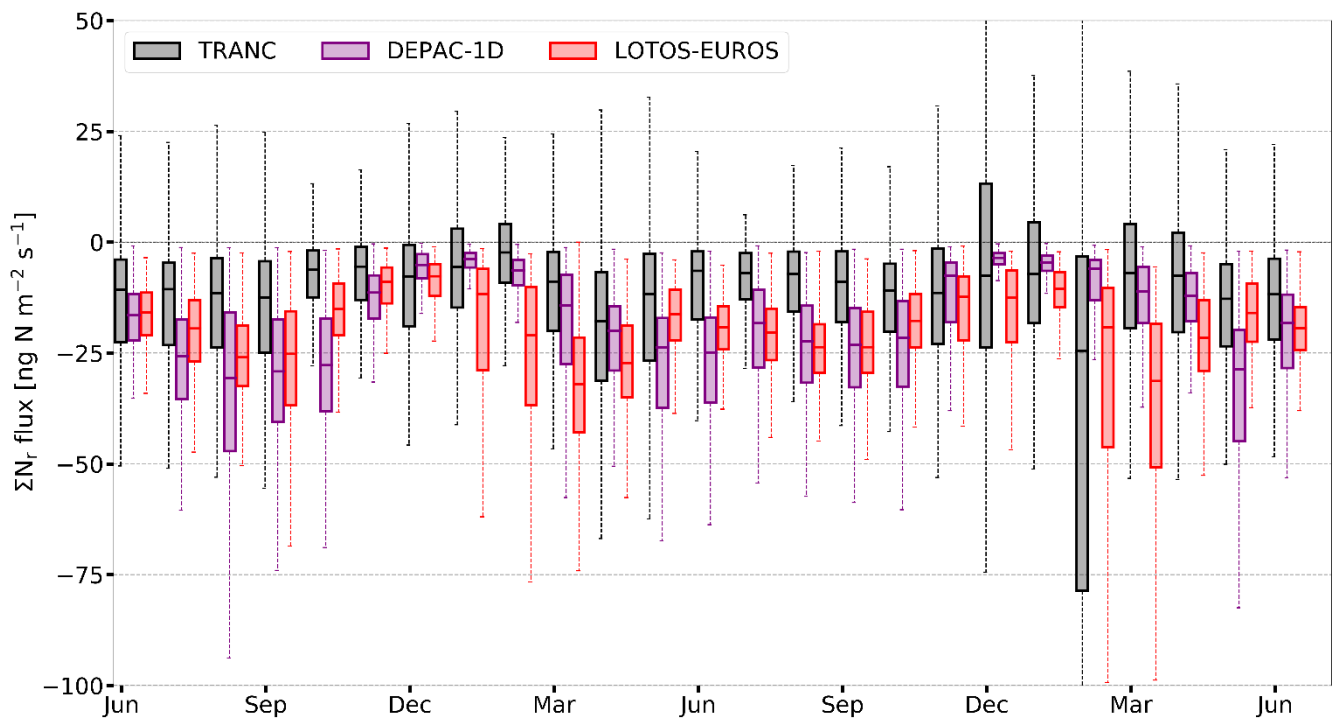
The largest discrepancy was found for NH₃ concentration as illustrated by Fig. 2 and S1 in detail. All of these investigated
input parameters play an important role in the modeling of the NH₃ exchange. In order to determine the impact of these
555 parameters on modeled NH₃ fluxes, we calculated NH₃ fluxes for the land-use class spruce forest with DEPAC-1D by replacing
a ~~certain specific~~ input parameter by its measured ~~entity counterpart~~ while all other input data were from LOTOS-EUROS.
Figure 5 illustrates the results of this comparison. Since modeled ~~temperature~~ and ~~measured values of~~ global radiation agreed
well ~~with their measured counterpart~~, deposition of NH₃ is only marginally reduced if measured values were used. Using
measured values of temperature as input parameter led to an increase in modeled NH₃ deposition by 0.82 kg N ha⁻¹, whereas
560 measured ~~r~~Relative humidity led to a ~~n increase~~ decrease in modeled NH₃ deposition by 0.80 kg N ha⁻¹, ~~but the effect is
constrained to approximately 6 %.~~ We found significant differences in ~~u_z u_{*}~~, but considering measured values in the flux
calculation leads only to a reduction by 1.3 kg N ha⁻¹ of 10%. As expected from the analysis of Fig. S6, NH₃ concentration
had the largest impact on deposition. Using measured NH₃ concentration reduced the deposition substantially by 42% 5.3 kg
565 N ha⁻¹ compared to using modeled concentrations. All reported differences refer to the entire campaign duration. ~~the modeled
deposition. As indicated by the lower panel, the largest discrepancy in fluxes was observed for the concentration case.~~



570 **Figure 5.** Comparison of NH₃ fluxes calculated with DEPAC-1D for the land-use class spruce forest based on measured (black) and modeled input data (red). The comparison was made for temperature, relative humidity, global radiation, friction velocity, and NH₃ concentrations. In the first row, NH₃ fluxes are shown as cumulative sums in kg N ha⁻¹. In the second row, scatter plots of NH₃ fluxes in ng N m⁻² s⁻¹ are given. Linear regressions are shown as black, solid lines, black, dashed lines represent 1:1 lines.

3.4.3.2 Comparison of modeled and measured ΣN_r deposition fluxes

575 The comparison of modeled ΣN_r fluxes with TRANC fluxes is presented in Fig. 6. Only periods during which high quality flux measurements were available were considered for the analysis. Models were basically able to capture the seasonal pattern of the ΣN_r fluxes well, but generally overestimated the measured flux amplitude. The ΣN_r exchange of DEPAC-1D is near zero during the entire winter, and thus the difference to measured deposition was nearly zero. During summer, a systematic overestimation of DEPAC-1D compared to measured fluxes was observed. Modeled deposition of LOTOS-EUROS was slightly lower than DEPAC-1D during summer and consequentially closer to measured fluxes. However, during autumn and spring predicted deposition of LOTOS-EUROS was significantly higher than deposition determined by DEPAC-1D and TRANC measurements due to the overestimated input NH₃ concentrations. Deposition was considerably high in LOTOS-EUROS. Similar observations were made during winter whereas median ΣN_r deposition of DEPAC-1D and TRANC was close to zero. Note that during February 2018 large-high aerosol concentrations were predicted both modeled and observed. The TRANC flux data also show the impact of the aerosol deposition, but to a larger extent as LOTOS-EUROS.



585 **Figure 6.** Fluxes of DEPAC-1D (purple), LOTOS-EUROS (red), and TRANC (black) from June 2016 to June 2018 shown as box-and-whisker plots. Whiskers of TRANC fluxes cover the range from -191 to 105 $\text{ng N m}^{-2} \text{s}^{-1}$ in February 2018; the upper whisker of December 2017 reached 69 $\text{ng N m}^{-2} \text{s}^{-1}$.

Figure S87 shows exemplarily monthly diurnal cycles of ΣN_r based on TRANC, DEPAC-1D, and LOTOS-EUROS. As previously written, during winter LOTOS-EUROS overestimated deposition whereas measurements showed near-zero exchange with occasional emission phases. From May to September/October, DEPAC-1D exhibited a clear diurnal pattern with lowest deposition during the night and highest values around noon, which was in line with results from TRANC measurements. However, fluxes were systematically overestimated as indicated by Fig. 6 and Fig. S87 during those months. During the same period, ΣN_r deposition of LOTOS-EUROS was lower but still higher than TRANC fluxes except for September. During that month, LOTOS-EUROS was similar to DEPAC-1D. Generally, the diurnal deposition pattern of

590

595 ~~LOTOS-EUROS was considerably dampened, thereby did not agreeing well with DEPAC-1D and TRANC. Compared to DEPAC-1D and TRANC measurements, deposition showed fewer diurnal variations resulting in a smaller daily amplitude.~~

3.45 Cumulative N exchange and method comparison

To derive annual deposition numbers the gap-filling procedures were applied to the time series of ~~the~~ TRANC and DEPAC-1D (see Sect. 2.12.3). Figure 7 shows the cumulative ΣN_r dry deposition of each method from January 2016 to end of June 2018. The contributions of the individual components to the dry ΣN_r deposition of DEPAC-1D were: 67.9 % NH_3 , 15.3 % HNO_3 , 10.4 % NO_2 , 5.2 % NH_4^+ , 1.0 % NO_3^- , and 0.1 % NO showing that modeled deposition was clearly driven by NH_3 . Since emission processes could only be treated for NH_3 , the observed emission of ΣN_r , for example ~~deduced for~~ in December 2017 (Wintjen et al., 2022), could not be sufficiently modeled. ~~Due to issues in the parametrization of stability in LOTOS-EUROS (see Sect. 4.2.2), particle deposition was enhanced in the LOTOS-EUROS results compared to DEPAC-1D (Fig. 7).~~

605 ~~Deposition of gases only was higher in DEPAC-1D due to the higher deposition velocities for NH_3 , NO_2 , and HNO_3 during summer compared to LOTOS-EUROS (Sect. 3.2.1). Comparing TRANC fluxes using MDV and DEPAC-1D in combination for gap-filling called TRANC(MDV+DEPAC-1D) to LOTOS-EUROS and DEPAC-1D, the differences in total dry deposition estimates were 5.4 and 2.8 kg N ha^{-1} after 2.5 years, respectively. ~~Total compensation point (Eq. 4) was on average at 0.024 $\mu\text{g N m}^{-2}$. Figure S8 shows the difference of ambient concentration and total compensation point for each month as boxplot.~~~~

610 ~~As seen by the whiskers, emission of NH_2 was possible only for certain periods in winter. Since NH_2 exchange was close to zero in winter, NH_2 emissions had hardly any influence on modeled total deposition of NH_2 . The disagreement to TRANC~~

deposition estimates was mainly related to the overestimation of ΣN_r fluxes in summer. Since the ΣN_r exchange was close to zero in winter, the difference to flux measurements was lower. As expected from the results above, LOTOS-EUROS exhibited a larger discrepancy to flux measurements. Still, modeled ΣN_r deposition was lower than by using DEPAC-1D in summer, but in relation to flux measurements relatively high in winter and spring as indicated by the slope of their cumulative curves and in Fig. 6 and Fig. S7. Due to the snow cover effect, particle deposition was higher in LOTOS-EUROS, whereas gaseous deposition was higher in DEPAC-1D.

615

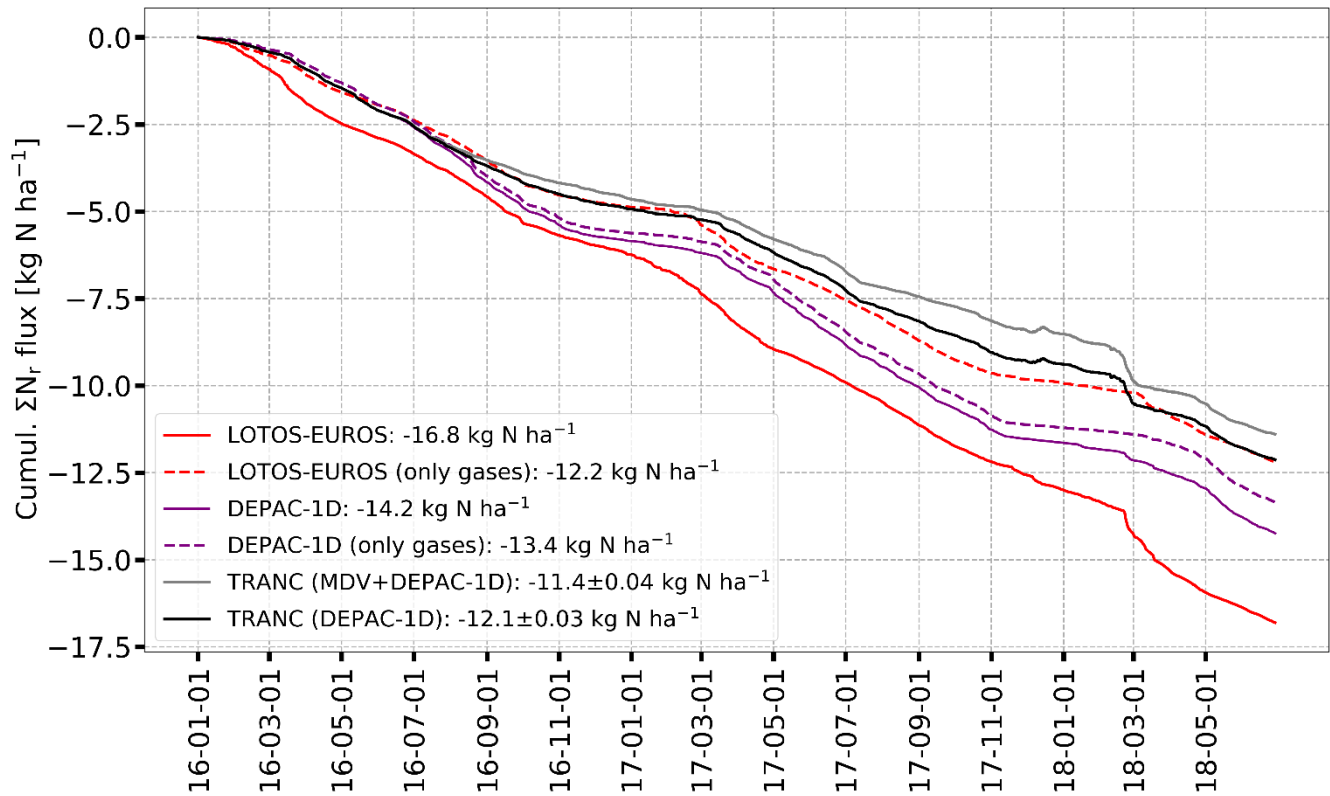


Figure 7. Comparison of measured and modeled cumulative ΣN_r dry deposition after gap-filling for the entire measurement campaign. Colors indicate different methods: TRANC+DEPAC-1D (black), TRANC+MDV+DEPAC-1D (grey), DEPAC-1D (purple), and LOTOS-EUROS (red). Dashed lines refer to cumulative dry deposition considering only gases. Number shown in the legend represent dry deposition and uncertainties after 2.5 years.

620

Both gap filling strategies resulted in similar deposition estimates. After 2.5 years, the difference was estimated to be in the order of 700 g N ha^{-1} . Uncertainties related to gap filling were negligible. Explicit differences in cumulative fluxes were found from June to September 2017 due to higher deposition fluxes in DEPAC-1D during those months. In February 2018, difference in measured deposition estimates was reduced since measured fluxes were larger than modeled fluxes of DEPAC-1D. Since all cumulative curves exhibit generally the same shape, we conclude that the variability in fluxes is reproduced by DEPAC-1D and LOTOS-EUROS well, although the amplitude and duration of certain deposition events is different. Furthermore, both gap-filling strategies resulted in similar deposition estimates showing that the application of MDV as gap-filling tool is reasonable. Uncertainties related to gap-filling measured TRANC time series by MDV and DEPAC-1D by Eq. (1) were negligible. In Fig. 8, a comparison of the ΣN_r dry deposition separated by methods and measurement years is shown. Corresponding values of the dry deposition estimates are given in Table 24.

630

Table 24. ΣN_r dry deposition of TRANC, DEPAC-1D, LOTOS-EUROS, and CBT for the entire measurement campaign, i.e., January 2016 to June 2018. Results from CBT were weighted according to the measured land-use weighting. For a visualization of the annual dry deposition see Fig. 8.

635

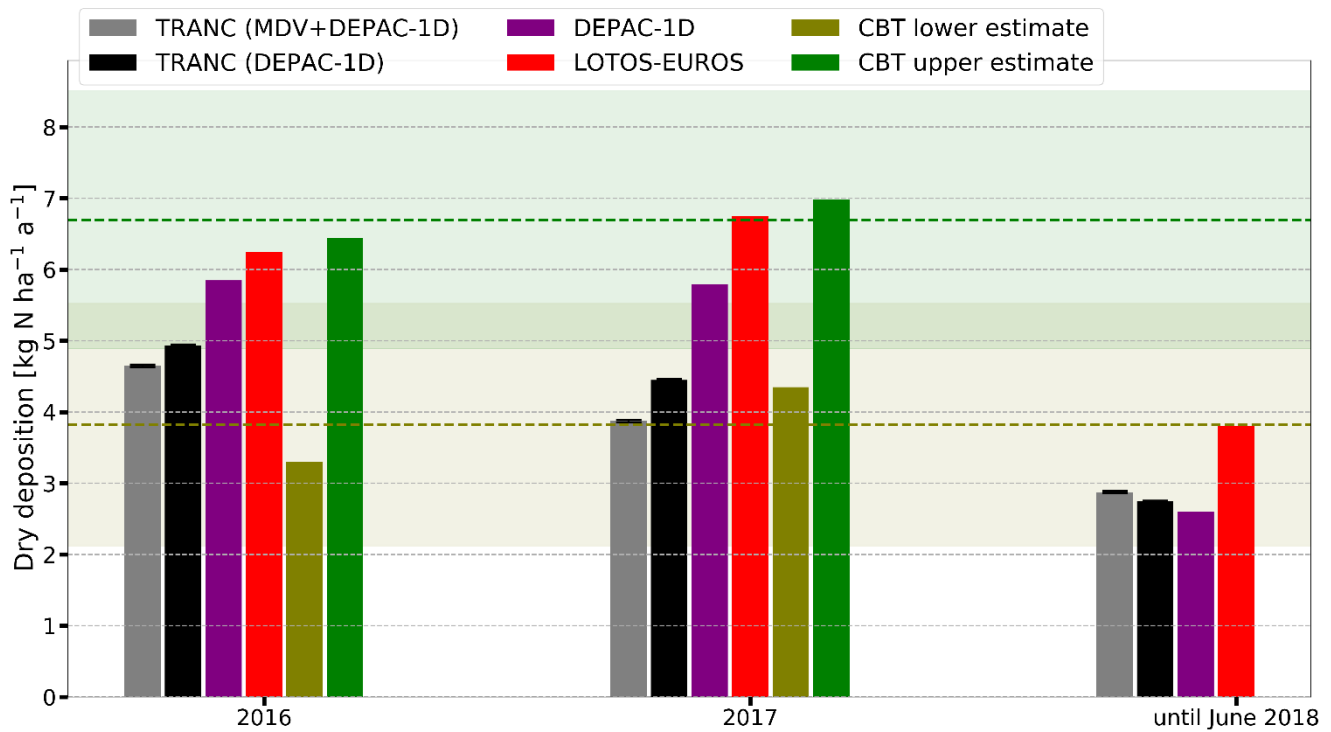
Method	2016 [$\text{kg N ha}^{-1} \text{ a}^{-1}$]	2017 [$\text{kg N ha}^{-1} \text{ a}^{-1}$]	until June 2018 [$\text{kg N ha}^{-1} \text{ a}^{-1}$]
TRANC (MDV+DEPAC-1D)	4.6	3.9	2.9
TRANC (DEPAC-1D)	4.9	4.5	2.7

DEPAC-1D	5.8	5.8	2.6
LOTOS-EUROS	6.2	6.8	3.8
CBT (lower estimate)	3.3	4.3	
CBT (upper estimate)	6.4	7.0	

In 2016, annual TRANC deposition was higher than in 2017. Using only DEPAC-1D as gap-filling technique, resulted in slightly higher dry deposition estimates. ~~However, differences were negligible compared to their total dry deposition estimates. Until June 2018, measured deposition was higher than the half of the previous years. DEPAC-1D deposition was nearly identical for 2016 and 2017, but lower than measured deposition until June 2018. In 2018, t~~ The difference to TRANC estimates until June 2018 was caused by the deposition fluxes in February 2018, which had an influence on the MDV method leading to significantly larger gap-filled fluxes. Hence, DEPAC-1D estimate was lowest among all methods for the first half of 2018. In 2016 and 2017, deposition estimates of DEPAC-1D were nearly identical due to similarities in micrometeorological and concentration input values. As expected from Fig. 7, annual LOTOS-EUROS estimates were highest in comparison to DEPAC-1D and TRANC. All deposition estimates were within the range of long-term lower and upper estimates of the CBT approach estimated from 2010 to 2018, with TRANC measurements close to the lower average and LOTOS-EUROS predictions to the higher average.

~~TRANC deposition was closer to the lower estimate of CBT, whereas DEPAC-1D predictions were within the standard deviation range of the CBT estimates. LOTOS-EUROS exhibited values close to the upper estimates of CBT. If we assume that the deposition from June to December 2018 would have been similar to the average of the previous measurement years (2.0, 2.3, 3.1, and 3.0 kg N ha⁻¹ a⁻¹ for TRANC (MDV+DEPAC-1D), TRANC (DEPAC-1D), DEPAC-1D, and LOTOS-EUROS, respectively), we would get dry deposition estimates similar to the previous years in case of TRANC and LOTOS-EUROS. DEPAC-1D estimates would be lower than 2016 and 2017. Annual dry deposition estimated by CBT were close to each other for 2016 and 2017 and in the range of the long-term averages estimated from 2010 to 2018 (3.8 kg N ha⁻¹ a⁻¹ as lower estimate and 6.7 kg N ha⁻¹ a⁻¹ as upper estimate).~~

Averaging of the annual sums of each method for 2016 and 2017 resulted in a TRANC dry deposition of 4.3 ± 0.4 and 4.7 ± 0.2 kg N ha⁻¹ a⁻¹ depending on the gap-filling approach. DEPAC-1D showed 5.8 ± 0.1 kg N ha⁻¹ a⁻¹, LOTOS-EUROS predicted 6.5 ± 0.3 kg N ha⁻¹ a⁻¹. We determined 6.7 ± 0.3 kg N ha⁻¹ a⁻¹ with CBT as averaged upper estimate, and 3.8 ± 0.5 kg N ha⁻¹ a⁻¹ as averaged lower estimate. ~~It shows that dry deposition estimated by TRANC, DEPAC-1D, and LOTOS-EUROS were within the minimum and maximum deposition estimated by CBT but generally closer to the lower estimate of CBT except for LOTOS-EUROS.~~



665

Figure 8. ΣN_r dry deposition for the years 2016 and 2017 and from January to June 2018 shown as bar chart. Colors indicate different methods: TRANC+(DEPAC-1D) (black), TRANC+(MDV+DEPAC-1D) (grey), DEPAC-1D (purple), LOTOS-EUROS (red), and canopy budget technique (olive and green). Data from TRANC, DEPAC-1D, and LOTOS-EUROS range from January 2016 to June 2018. CBTs' lower and upper estimates weighted according to the measured land use. The colored dashed lines indicate the averaged dry deposition of the lower and upper estimates (dashed, brown line and dashed, olive line, respectively) were from 2010 to 2018, the shaded areas represent their standard deviation.

670

4 Discussion

4.1 Comparison of concentrations, fluxes, and annual budgets

675

The comparison to concentration measurements of NO , NO_2 , and NH_3 conducted by Wintjen et al. (2022) revealed that NH_3 concentrations were systematically overestimated by LOTOS-EUROS during the entire campaign as described in Sec. 3.1 in detail. Modeled NO_x concentrations were similar or even lower than their measured values. Modeled seasonal patterns of NO_x and NH_3 agreed partly with their observed pendants. In case of NO_x , model and measurements reported highest values in winter and lowest values in summer mostly related to differences in emissions from enhanced heating and combustion processes. In case of NH_3 , a peak in the LOTOS-EUROS concentrations was found during spring. However, the predicted increase in NH_3 during autumn was not confirmed by the observations. Elevated NH_3 concentrations were most likely related to emissions from agriculture, in particular to the application of fertilizer during these times. Thus, the low pollution climate at the site could not be modeled well by LOTOS-EUROS.

680

685

Compared to other forest ecosystems, modeled concentrations of LOTOS-EUROS were closer to reported concentrations, e.g. for HNO_2 (Farmer et al., 2006; Horii et al., 2006; Farmer and Cohen, 2008), for NH_3 (Wyers and Erisman, 1998; Hansen et al., 2013, 2015), for NO_3^- and NH_4^+ (Wolff et al., 2010; Gordon et al. 2011; Farmer et al. 2011, 2013), and NO_2 (Horii et al., 2004; Farmer and Cohen, 2006).

Differences in the concentration contribution of N_r species to ΣN_r

690

According to the LOTOS-EUROS simulations, NH_3 had a predominant role in the ΣN_r concentration pattern. This result was in contrast to concentration measurements of individual N_r species at the site highlighting NO_x as the prevailing compound in the concentration pattern of ΣN_r (Wintjen et al., 2022). Moreover, the comparison of absolute concentration values revealed that NH_3 was overestimated by LOTOS-EUROS explicitly during spring, and seasonal patterns of NH_3 did not agree for some

periods like in autumn. NO_x concentrations agreed well in their seasonal pattern, but modeled concentrations were systematically lower.

695

The predominant role of NH_3 in the modeled concentrations is caused by the emission inventory used in this study. The emission inventory spatially allocates NH_3 manure derived emissions through a procedure in which the animal numbers per region and agricultural land within a region are the two proxies used. Emissions from fertilizer application are allocated solely on land use. Hence, within a region all agricultural land is assumed to emit the same amount of NH_3 , although the intensity of the agricultural practice and distribution of housing may vary substantially within such a region. Only south of the site, agricultural lands are located within $7 \times 7 \text{ km}^2$ model resolution representing the site. This means that in the grid cell of the model, in which the station is located, there is an emission source contributing an increased NH_3 concentration even when the wind directions are not transporting air from this agricultural region towards the station.

700

705

In LOTOS-EUROS, particulate nitrogen also had a significant contribution to modeled ΣN_r , which could not be confirmed by measurements. However, the comparison of particulate nitrogen concentrations is difficult because of the aerosol cut-off size in DELTA measurements being at $4.5 \mu\text{m}$ (Tang et al., 2015). Aerosols available in fine mode like ammonium sulfate ($(\text{NH}_4)_2\text{SO}_4$) and ammonium nitrate (NH_4NO_3) are associated with aerodynamic diameter of less than $2.5 \mu\text{m}$ (Kundu et al., 2010; Putaud et al., 2010; Schwarz et al., 2016) and could be sufficiently sampled. Concentrations of coarse-mode aerosols with larger diameters than the cut-off size were partly underestimated. However, concentrations of sodium, magnesium, and calcium ions were negligible at the site (Wintjen et al., 2022) indicating that coarse-mode nitrate aerosols had no significant contribution to ΣN_r concentration. In addition, carbonate coated denuders used for collecting HNO_3 overestimate concentrations by approximately 45 % since nitrous acid also sticks to those prepared surfaces (Tang et al., 2021). Thus, disagreements could be related to emission inventory of $\text{PM}_{2.5}$ and PM_{10} , chemical process modeling, or to DELTA measurements.

710

715

NO_x concentrations agreed in their seasonal dynamics, thus processes responsible for modeling temporal dynamics of NO_x emissions are implemented reasonably in LOTOS-EUROS. However, the systematic underestimation of NO_x concentration by LOTOS-EUROS shows that NO_x sources within this grid cell, most likely emissions from road transport and private households due to the absence of large industrial areas or power plants in the surroundings of the station, are presumably not tracked sufficiently by the emission inventory.

720

Generally, the low measured concentrations of N_r compounds show that the site was mostly outside the transport range of nitrogen enriched air masses. Improvements in the close-range transport in LOTOS-EUROS regarding atmospheric lifetime of N_r species or in the definition of atmospheric layers are likely needed. A reduction in grid cell size could lead to a more accurate localization of potential nitrogen emission sources and a better description of close-range transport and dilution effects. The impact of an increase in model resolution is elaborated in Sect. 4.2.2.

725

Differences in measured and modeled ΣN_r fluxes

730

Overall, measured and modeled ΣN_r deposition were comparable in the order of magnitude and partly agreed in temporal dynamics but still exhibited disagreements in flux amplitude, which were related to differences in concentration, micrometeorology, and the integration of exchange pathways in DEPAC. Currently, a compensation point is only implemented for NH_3 , and thus only deposition fluxes could be modeled for other compounds. Since the total compensation point of NH_3 was negligible in DEPAC, emission fluxes of NH_3 observed for a deciduous forest by Hansen et al. (2015) probably due to a

735 decay of fallen leaves (Hansen et al., 2013) could not be reproduced. The soil compensation point, which is integrated in the calculation of the NH_3 compensation point but currently set to zero, may reduce the observed differences to TRANC fluxes.

In case of NO_2 , no compensation point is implemented, and deposition on leaves is hardly allowed. Both assumptions are in disagreement with findings by Horii et al. (2004), who identified non-stomatal deposition as strongest contributor to the flux, and by Thoene et al. (1996), who proposed the existence of a compensation point for NO_2 . However, nitrogen concentrations in leaf samples taken in surroundings of the site showed no unusually high enrichment of nitrogen in leaves and needles (Beudert and Breit, 2014). Thus, neglecting the emission pathway of oxidized nitrogen compounds like NO_2 seems reasonable for the measurement site.

745 To reduce the difference between measured and modeled fluxes, considering nitrogen emissions from soil may lead to a closer agreement with flux measurements. As written above, soil compensation point has no influence on deposition of N_r species in DEPAC yet, and soil resistance implementation is kept simple: A constant value is assumed depending on the soil wetness (dry, wet, or frozen). Improvements in the description of the exchange with the soil surface may allow to describe the observed TRANC emission fluxes in December 2017 reported by Wintjen et al. (2022). Changes made to the soil exchange path may lower the flux contribution of NH_3 as outlined before but increase the contribution NO since the latter is generally observed as emission from soil if it is produced through (de)nitrification processes (Butterbach-Bahl et al., 1997; Rosenkranz et al., 2006). At the reference height, contribution of NO may be still low due to fast conversion processes to NO_2 in the presence of ozone (O_3) within the forest canopy, especially close to the ground (Rummel et al., 2002; Geddes and Murphy, 2014). Increased NO_2 concentrations within the forest canopy may alter concentrations of various N_r species, e.g., resulting in the formation of HNO_3 , which may contribute substantially to the deposition flux (Munger et al., 1996; Horii et al., 2006). Consequently, a soil compensation point may be also relevant for the exchange of other N_r species next to NH_3 .

~~Modeled NH_2 fluxes were similar to observations of Hansen et al. (2015) ranging from -60 to $120 \text{ ng N m}^{-2} \text{ s}^{-1}$ above a deciduous forest. The emission fluxes observed by Hansen et al. (2015) were probably caused by the decay of fallen leaves (Hansen et al., 2013) leading to less deposition during late summer and autumn compared to our site. During spring, Pryor et al. (2001) reported a daily deposition of $15 \text{ ng N m}^{-2} \text{ s}^{-1}$ for NH_3 , which was comparable to predicted median depositions of DEPAC 1D and LOTOS EUROS in the same season although ambient NH_3 concentrations were different. The high contribution of emission fluxes observed by Hansen et al. (2015) was not reproduced by the model applications at our site, which was probably related to the negligible compensation point of NH_3 . Since no compensation point is implemented for other N_r compounds, only deposition fluxes could be modeled for those compounds. In addition, their flux amplitude was significantly lower than for NH_3 . Thus, the combined ΣN_r flux was mainly controlled by the NH_3 flux pattern.~~

~~Unlike NH_3 , modeled NO fluxes had an insignificant contribution to the ΣN_r flux. Geddes and Murphy (2014) found that NO fluxes were mostly downward with a maximum deposition of $2.9 \text{ ng N m}^{-2} \text{ s}^{-1}$ during daytime. The diurnal cycle of NO was reversed to NO_2 during the day and was nearly zero with a tendency of slight emission during the night (Horii et al., 2004; Geddes and Murphy, 2014). Thus, they observed emission of NO_2 during the day peaking at approximately $2.8 \text{ ng N m}^{-2} \text{ s}^{-1}$. As a result, NO_x fluxes were slightly different from zero. Horii et al. (2004) found NO_2 deposition at concentrations higher than $1.1 \text{ } \mu\text{g N m}^{-2}$ and emission fluxes in the opposite case. They further identified non-stomatal deposition as the strongest contributor to the flux. Min et al. (2014) observed emission fluxes for NO and NO_2 during daytime but with even lower flux amplitude. Besides the emission fluxes, modeled deposition fluxes of NO_2 and NO were within the range of the reported values.~~

The contribution of NO to total modeled ΣN_x dry deposition was negligible due to the high canopy resistance implemented in DEPAC. In general, NO is mainly observed as emission from soil if it is produced through (de)nitrification processes (Butterbach-Bahl et al., 1997; Rosenkranz et al., 2006). Most of the NO is rapidly converted to NO₂ in the presence of ozone (O₃) within the forest canopy, especially close to the ground (Rummel et al., 2002; Geddes and Murphy, 2014). Thus, NO fluxes were assumed to be close to zero in DEPAC at the reference height due to fast conversion processes within the forest canopy and uptake possibilities like leaf surfaces for N_x compounds (e.g., Wyers and Erisman, 1998; Rummel et al., 2002; Sparks et al., 2001; Gordon et al., 2011; Geddes and Murphy, 2014; Min et al., 2014; Wentworth et al., 2016).

It has to be considered that NO₂ is removed from the atmosphere by the reaction with O₃. During the night, NO₂ reacts with NO₂ to dinitrogen pentoxide (N₂O₅). The latter can react with H₂O to HNO₃. HNO₃ as well as peroxyacetyl nitrates (PANs) (Min et al. 2014) are effective sinks for NO₂, and HNO₃ has a significant impact on the measured deposition flux (Munger et al., 1996). Modeled HNO₃ fluxes had a similar flux magnitude as the NO₂ fluxes. Comparing predicted HNO₃ fluxes with values reported for different forest sites shows that HNO₃ was predominantly deposited at selected sites (see Walker et al., 2020, Table 1) with values ranging from 1.4 to 40 ng N m⁻² s⁻¹ depending on forest types and time of the year. Modeled HNO₃ fluxes were at the lower end of published values.

Horii et al. (2006) reported inferred HNO₃ fluxes almost as high as the measured total NO_x fluxes. NO_x corresponds to the sum of all oxidized nitrogen compounds, for example, NO, NO₂, particulate NO₃⁻, HNO₃, N₂O₅, PAN, and other organic nitrates. Their measured NO_x deposition ranged between 0 and 80 ng N m⁻² s⁻¹. Comparing the values of NO_x and HNO₃ summarized by Walker et al. (2020) shows that HNO₃ fluxes were almost as high as the NO_x fluxes highlighting their relevance in the NO_x flux budget.

Modeled NO₃⁻ and NH₄⁺ deposition fluxes were similar in magnitude and their absolute flux values were mostly below 1 ng N m⁻² s⁻¹ considering their flux medians. NH₄⁺ fluxes were similar to values reported by Farmer et al. (2011), who observed NH₄⁺ deposition with 1 ng N m⁻² s⁻¹ at maximum for a coniferous forest during midday. Gordon et al. (2011) found an average NO₃⁻ flux of 0.8 ng N m⁻² s⁻¹ with a standard deviation of 1.5 ng N m⁻² s⁻¹. Wolff et al. (2010) conducted measurements of total ammonium (NH₃ and NH₄⁺) and total nitrate (HNO₃ and NO₃⁻) above a spruce forest. They determined mean fluxes of 66 ng N m⁻² s⁻¹ and 41 ng N m⁻² s⁻¹ for tot NH₄⁺ and tot NO₃⁻, respectively. Modeled tot NH₄⁺ and tot NO₃⁻ of LOTOS-EUROS were significantly lower. Monthly medians ranged between 2.9 and 26.3 ng N m⁻² s⁻¹ and between 0.74 and 4.0 ng N m⁻² s⁻¹ for tot NH₄⁺ and tot NO₃⁻, respectively. Similar values were calculated for DEPAC-1D.

In conclusion, modeled deposition fluxes are comparable to flux measurements conducted at various forest ecosystems. However, comparison possibilities to flux measurements of N_x compounds, e.g., NH₃ and particles (Walker et al., 2020), above forests are still sparse. In addition, most of the studies were carried out for a limited time of the year. The comparison revealed that emission fluxes were observed for NH₃ and NO₂ due to the existence of a compensation point, the alternation of day and night, or changes in surface properties or micrometeorology.

The comparison to TRANC fluxes indicated an overestimation of modeled ΣN_x . Predicted ΣN_x fluxes of DEPAC-1D were systematically higher in summer, and LOTOS-EUROS ΣN_x deposition was suspiciously high in winter whereas measured and site-based fluxes were close to zero. Median ΣN_x of TRANC and LOTOS-EUROS were close to each other and lower than DEPAC-1D for the entire campaign. Except for NH₃ and nitrogen aerosols, LOTOS-EUROS and DEPAC-1D gave similar values for each compound (Fig. 3). In case of TRANC measurements, significant emission fluxes were found in winter as discussed in Wintjen et al. (2022) for December 2017. Generally, emissions could not be sufficiently reproduced by the models

~~since emissions from soil are currently not included in DEPAC.~~ The observed large deposition fluxes in February 2018 were reproduced in the model simulations although the modeled flux amplitude was smaller. During that time, modeled concentrations and fluxes of particulate N_r were the largest contributor to total ΣN_r , leading to the assumption of particle driven ΣN_r deposition. DELTA measurements suggested that particulate NH_4^+ was most likely responsible for the measured ΣN_r deposition (Wintjen et al., 2022, Fig. 10). Modeled and measured NH_4^+ concentrations differed only by $0.75 \mu g N m^{-3}$ whereas a significant disagreement was found between NH_3 measurements and LOTOS-EUROS (approx. $2.7 \mu g N m^{-3}$). According to DELTA measurements, the NH_3 concentration was approximately $0.17 \mu g N m^{-3}$. The averaged SO_2 concentration obtained from LOTOS-EUROS and DELTA were comparable during the exposure period of the samplers (1.5 and $2.0 \mu g m^{-3}$, respectively). According to the LOTOS-EUROS simulations, an excess of pNH_4^+ over pNO_3^- was modeled suggesting that particle deposition was most likely caused by pNH_4^+ , which is in agreement with DELTA measurements. ~~In case of the LOTOS-EUROS simulations, the dominant aerosol could have been NH_4NO_3 due to the high NH_3/SO_2 ratio. (Trebs et al., 2005).~~ In conclusion, the high deposition fluxes seem to be driven by particulate NH_4^+ compounds, ammonium sulfate and ammonium nitrate. During February 2018, DELTA measurements revealed a slightly lower concentration of the SO_4^{2-} than the NO_3^- aerosol, 1.28 and $1.63 \mu g m^{-3}$, respectively, suggesting that NH_4NO_3 was most responsible ~~as the aerosol likely responsible~~ for the ~~measured~~ observed ΣN_r deposition fluxes. Still, the dominant aerosol is not fully known due to missing high-resolution measurements of nitrogen aerosols. Apart from February 2018, winter fluxes of LOTOS-EUROS were large compared to DEPAC-1D although the same size-resolved model for determining aerosol deposition velocities was used. By comparing dry deposition caused by gases+particles and gases only of DEPAC-1D and LOTOS-EUROS (Fig. 7), a substantial disagreement in aerosol deposition was found. The large particulate nitrogen fluxes of LOTOS-EUROS are caused by uncertainties in the stability parametrization (Sect. 4.2.2).

Analysis of ΣN_r deposition estimates

The ΣN_r dry deposition estimates of TRANC, DEPAC-1D, and LOTOS-EUROS were in the same range after 2.5 years but differences in seasonal flux patterns were found. ~~The annual dry deposition estimates of all methods were in the same range considering uncertainties of measured fluxes and model applications (see Sect. 4.2 and 4.3). Annual estimates from TRANC were lower than the results from DEPAC-1D and LOTOS-EUROS. The reasons for the differences to the modeling approaches were elaborated in the previous sections. Possible uncertainties regarding model applications are described in the subsequent sections. Uncertainties in TRANC measurements were discussed in Sect. 4.3 of Wintjen et al. (2022). At the measurement site,~~ In addition, both gap-filling methods applied to flux measurements led to similar dry deposition estimates indicating that the MDV approach is suitable for gap-filling of short-term gaps in TRANC flux timeseries. During summer, we found differences in the gap-filled fluxes due to ~~the~~ systematic overestimation of DEPAC-1D, which was related to the different response of DEPAC-1D to micrometeorological conditions compared to TRANC (Fig. 4). It should be kept in mind that monthly integrated pNO_3^- , pNH_4^+ , and HNO_3 ~~were measured by long-term samplers and monthly~~ concentration estimates may not be able to fully ~~representative capture of~~ local events. Moreover, the aerosol cut-off size of DELTA was probably lower than of the TRANC measurements as supposed by Wintjen et al. (2022). Saylor et al. (2019) also noted that v_d of particles for forest are highly uncertain. Thus, differences to measurements and predictions of LOTOS-EUROS in particle deposition could be expected. Besides missing emission fluxes in DEPAC-1D, the agreement of the dry deposition estimates was reasonable ~~showing~~ indicating that an inferential model like DEPAC-1D ~~as an~~ can be a valuable alternative to purely statistical ~~alternative~~ gap-filling tool at sites or seasons with predominant N deposition.

Annual dry deposition estimates from TRANC, LOTOS-EUROS, and DEPAC-1D were found to be within the range of the lower and upper estimates of the CBT approach. Adding the wet-only deposition results reported in Wintjen et al. (2022) to

determined dry depositions, we calculated annual total depositions ranging between 11.5 and 14.8 kg N ha⁻¹ a⁻¹ noted in Table 2-3 for each year.

865 **Table 3-2** Annual ΣN_r deposition of TRANC, DEPAC-1D, LOTOS-EUROS, and CBT for 2016, 2017, and from January to June 2018 in kg N ha⁻¹ a⁻¹. Wet-only depositions of NO₃⁻, NH₄⁺, and DON were adapted from Wintjen et al. (2022).

Method	2016 [kg N ha ⁻¹ a ⁻¹]	2017 [kg N ha ⁻¹ a ⁻¹]	Until June 2018 [kg N ha ⁻¹ a ⁻¹]
TRANC (MDV+DEPAC-1D)	12.9	11.7	6.3
TRANC (DEPAC-1D)	13.1	12.3	6.2
DEPAC-1D	14.1	13.6	6.1
LOTOS-EUROS	14.4	14.6	7.3
CBT (upper estimate)	11.5	12.2	
CBT (lower estimate)	14.6	14.8	

Comparing the results obtained from the measurement site to results obtained for other forest ecosystems using a similar validation procedure is rather difficult due to a large temporal and spatial variability in N_r compounds contributing to ΣN_r. Additionally, micrometeorological measurements as carried out in this study require substantial effort in maintenance and processing of the acquired data. Thus, most currently available EC measurements are limited to time periods covering a few weeks or months and are only available for certain locations.

875 Recently, Ahrends et al. (2020) compared deposition estimates of a CBT approach, an inferential method, and LOTOS-EUROS for several forest ecosystems. However, their CBT based on the variant suggested by Ulrich (1994), which is different to the version used in this study, and their inferential method (IFM) was only applied to NO₂ and NH₃ due to the limited availability of ambient concentration measurements for other N_r compounds. In addition, deposition velocities for NO₂ and NH₃ were calculated based on literature research for different forest types accompanied by various correction factors. They reported similar annual dry deposition estimates for CBT and IFM, which were found to be 12.6 and 12.9 kg N ha⁻¹ a⁻¹, respectively. 880 Minimum dry deposition was 3.8 kg N ha⁻¹ a⁻¹ for CBT and 1.0 kg N ha⁻¹ a⁻¹ for IFM. The lowest average dry deposition was 9.3 kg N ha⁻¹ a⁻¹ given by LOTOS-EUROS but its minimum dry deposition was highest (approx. 6.3 kg N ha⁻¹ a⁻¹). Since we measured N deposition in a low-polluted environment, the agreement to the minimum dry deposition estimates of Ahrends et al. (2020) seems reasonable.

885 In the consideration of critical loads, total nitrogen deposition is ~~close within to~~ the proposed limits. Critical loads ranging from 10 to 15 kg N ha⁻¹ a⁻¹ and 10 to 20 kg N ha⁻¹ a⁻¹ were defined by Bobbink and Hettelingh (2011) for *Picea abies* and *Fagus sylvatica*, respectively. Since *Picea abies* was the prevailing tree species in the flux footprint (approx. 80%), the critical load of the investigated forest ecosystem is probably closer to the limits of *Picea abies*. ~~Thus, the investigated forest ecosystem is in a potentially endangered state.~~ The state of tree physiological parameters suggested that the critical load concept, which 890 indicated that the exposure of the forest to N deposition is still below critical limits, is a valuable tool to evaluate the functionality of an ecosystem. Long-term observations of nitrogen input to this ecosystem showed nitrogen concentrations in trees and water reservoirs, but ecosystem functionality was not impaired. According to leaf examinations done by Beudert and Breit (2014) at the site, balanced ratios of nitrogen to other nutrient concentrations in tree foliage were found, and usual tree growths were reported. Jung et al. (2021) found low nitrate concentrations in soil water, aquifers, and streams at the site 895 showing an intact nitrogen retention and storage system. Moreover, green algae coatings on spruce needles usually indicating higher NH_x dry deposition (Grandin, 2011) were not found at the site. ~~It should be kept in mind that this result refers to the current climatic situation and concentration level of various N_r compounds. Additionally, nitrogen input to the atmosphere on a broader scale will probably increase due to a growing population for which food security needs to be ensured. However, if~~

900 proposed mitigation strategies on air pollutants, e.g., O₃ and NO₂, are successfully implemented in Europe, reductions in these gases could be still achieved even if global temperatures will rise by 2°C (Watson et al., 2016). Recently, van Damme et al. (2021) found that atmospheric NH₃ concentrations increased on different continents considering the years 2008 to 2018. Exceedances of critical loads could be still possible for forest ecosystems even at remote locations in the future.

4.2 Modeling uncertainties

905 *Influence of micrometeorological parameters*

In both DEPAC-1D and LOTOS-EUROS, wet leaf surfaces and high relative humidity were identified as conditions enhancing ΣN_r deposition from May to September. In case of temperature, dry leaf surfaces, and low relative humidity, diurnal cycles of v_d showed a different behavior: For DEPAC-1D, lower temperatures were found to increase v_d , whereas the opposite observation was made for LOTOS-EUROS and their shapes were different. Deposition velocities of DEPAC-1D reached 910 highest values around noon and decreased towards evening. LOTOS-EUROS predicted highest values in the morning and evening, but deposition velocities exhibited a decreasing trend towards noon. These disagreements were probably related to the stomatal uptake of NH₃ prevailing in the ΣN_r deposition flux of LOTOS-EUROS. Only for wet leaf surfaces and high relative humidity, which generally hold an important role in the deposition of NH₃ (Wentworth et al., 2016), diurnal shapes of DEPAC-1D and LOTOS-EUROS were similar suggesting that cuticular deposition of NH₃ seemed to be most responsible for 915 the modeled ΣN_r dry deposition at the measurement site. Similar observations were made by Wyers and Erisman (1998), who identified the cuticular pathway as a larger sink for NH₃ than the stomatal pathway.

However, the results from TRANC measurements highlighted higher temperatures, lower relative humidity, and dry leaf surfaces as important factors enhancing ΣN_r deposition, and diurnal cycles of the TRANC were different in shape from those 920 of LOTOS-EUROS. In addition, night-time deposition velocities of the TRANC were close to zero, whereas modeled deposition velocities were between 0.5 and 1 cm s⁻¹. The differences are probably related to low aerodynamic resistances in the model applications indicating high u_* values, which could not be verified by EC measurements. However, measuring night-time exchange with the EC method and micrometeorological methods in general is challenging. Common detection algorithms for a u_* threshold (Reichstein et al., 2005; Barr et al., 2013) are not applicable to N_r species yet since they are optimized for 925 CO₂. The contradiction in wet and dry conditions lead to the assumption that the current implementation of the NH₃ exchange pathways in DEPAC was not fully suited for predicting NH₃ deposition correctly and needs further investigation. It should be kept in mind that we measured ΣN_r exchange at a low-polluted, mixed forest site. Sites with different micrometeorology, vegetation, and pollution climate may exhibit other parameters like surface wetness, canopy temperature, and ambient concentration responsible for the ΣN_r exchange as found by Milford et al. (2001). Further comparisons to flux measurements 930 of ΣN_r and NH₃ are needed to investigate the role of stomatal and cuticular deposition.

Influence of soil resistance and soil compensation point

In DEPAC, soil resistance is set to a constant value depending on soil status, i.e. frozen ($R_{soil}=1000$ s m⁻¹), dry ($R_{soil}=100$ s m⁻¹), or wet ($R_{soil}=10$ s m⁻¹). In addition, the in-canopy resistance (as part of the effective soil resistance) is dependent on the 935 inverse of u_* , surface area index (LAI+ area index of stems and branches (van Zanten et al., 2010)) and may lower the exchange with the soil. A soil compensation point is currently set to zero for NH₃ and not implemented for other N_r species since an appropriate parametrization or value is not known so far as argued by van Zanten et al. (2010). Consequently, deposition through the soil pathway is close to zero for most half-hourly records according to the current parametrization. Including a soil compensation point in DEPAC and improvements in the soil resistance parametrization, may lead to a better agreement with 940 flux measurements. However, modifications related to soil exchange are probably challenging since they may affect the

contribution of various N_r species to the ΣN_r flux, and a parametrization of soil resistance, e.g., depending on soil moisture and temperature, is probably required instead of assuming a constant value.

945 At the site, no measurements of soil conductance, soil moisture, and soil temperature were made. Thus, we cannot evaluate the representativeness of the current soil parametrization. Moreover, those measurements would have been challenging at the site due to the large spatial variability in the wide flux footprint area. For further measurement campaigns of similar nature, measurements of soil specific parameters are highly recommended.

4.2 Uncertainties in DEPAC-1D

950

~~We identified wet leaf surfaces, high relative humidity, and lower temperatures as conditions enhancing ΣN_r deposition from May to September. Wet conditions hold an important role in the deposition of NH_3 (Wentworth et al., 2016) and cuticular deposition was identified as a larger sink for NH_3 than stomatal deposition (Wyers and Erisman, 1998). However, the results from TRANC measurements highlighted higher temperatures, lower relative humidity, and dry leaf surfaces as important factors enhancing ΣN_r deposition (Wintjen et al., 2022). Wet conditions, likely enhancing cuticular deposition of NH_3 , seemed to be most responsible for the ΣN_r deposition at the measurement site as suggested by the models. The contradiction in wet and dry conditions lead to the assumption that the current implementation of the NH_3 exchange pathways in DEPAC was not fully suited for predicting NH_3 deposition correctly under all site characteristics and situations and needs further investigation. It should be kept in mind that we measured ΣN_r exchange at low polluted, mixed forest site (Beudert and Breit, 2010; Wintjen et al., 2022). Sites with different micrometeorology, vegetation, and pollution climate may exhibit other parameters like surface wetness, canopy temperature, and ambient concentration responsible for the ΣN_r exchange as found by Milford et al. (2001). Further comparisons to flux measurements of ΣN_r and NH_3 are needed to investigate the role of stomatal and cuticular deposition.~~

960

Cuticular compensation point of NH_3

965 Schrader et al. (2016) discovered problems in the calculation of the cuticular NH_3 compensation point under high ambient NH_3 concentrations and high temperatures, for instance during summer. The current implementation of Wichink Kruit et al. (2010) in DEPAC likely underestimates the cuticular compensation point at high temperatures. This issue is not solved yet and could not be verified for our measurement site due to generally low NH_3 concentrations and the implementation of monthly averaged NH_3 concentration instead of half-hourly values in the concentration time series of NH_3 to some extent. ~~However, NH_3 concentration were rather low at the measurement site, and~~ Moreover, the cuticular emission potential was estimated from monthly averaged concentrations in LOTOS-EUROS and DEPAC-1D, instead of instantaneous values as in the original parameterization of Wichink Kruit et al. (2010), likely somewhat alleviating the issue discussed in Schrader et al. (2016). Thus, this issue could not be not the main reason for the difference to flux measurements at our site. ~~Unfortunately, NH_3 flux calculation with the EC method was not possible at the measurement site. No distinct time lag was found during the entire measurement campaign. Presumably, variability in measured raw concentrations of NH_3 could not be adequately identified by the NH_3 QCL (Ferrara et al., 2021; Wintjen et al., 2022).~~

970

975

Influence of emission fluxes on ΣN_r

980 With the TRANC system, the contribution of ΣN_r emission fluxes above the limit of detection was estimated to 16 % (Wintjen et al., 2022). Unfortunately, robust QCL-based NH_3 flux measurements using the EC method were not possible at the measurement site (Wintjen et al., 2022). Thus, contribution of individual N_r species – at least the NH_3 and hence the reduced N contribution - to the measured ΣN_r flux is not known. However, the presence of emission fluxes shows that an implementation of a compensation point for soil and/or mechanisms describing emissions of oxidized N_r species like NO_2 and

HNO₃ should be considered. As described above, fully integrating the soil compensation point in the exchange of NH₃ may explain emissions fluxes of ΣN_r. In case of HNO₃, a constantly, low R_{so} is assumed leading to a median v_d similar to NH₃ since median R_{so} of NH₃ was about 15 s m⁻¹ for the entire campaign. In general, deposition velocities of NH₃, HNO₃, NO₂, and NO proposed by the Association of German Engineers (VDI, 2006) were generally larger than modeled medians (see Fig. 3). Deposition velocity of NH₃ was in the range of values reported by Schrader and Brümmer (2014) for mixed forests. In addition, Horii et al. (2006), Pryor and Klemm (2004), and Farmer and Cohen (2008) found deposition velocities for HNO₃ similar to our results. However, emissions for For HNO₃, emission fluxes were reported in recent publications (Tarnay et al., 2002; Farmer and Cohen, 2006, 2008). The latter conducted flux measurements of HNO₃ above a pine forest and found a significant contribution of emission fluxes during summer. Those emission could also be induced by the evaporation of NH₄NO₃ from leaf surfaces occurring at higher temperatures (Wyers and Duyzer, 1997; Van Oss et al., 1998), by interactions with hydrochloric acid, or particles deposited or formed on leaf surfaces as discussed by Nemitz et al. (2004). Deposition velocities for NO and NO₂ were in agreement with values reported in several studies, e.g., mostly ranging between 0.005 and 0.012 cm s⁻¹ for NO (Delaria, et al., 2018) and between 0.015 and 0.51 cm s⁻¹ for NO₂ (e.g., Rondon et al., 1993; Horii et al., 2004; Chaparro-Suarez et al., 2011; Delaria, et al., 2018, 2020). However, emission fluxes of NO and NO₂ were reported in several publications, e.g., Farmer and Cohen (2006), Horii et al. (2004), and Min et al. (2014) leading to the assumption of the existence of a compensation point (Thoene et al., 1996), whereas other authors but a compensation point for NO and NO₂ is still critically under discussion such a compensation point for NO and NO₂ (Chaparro-Suarez et al., 2011; Breuninger, et al. 2013; Delaria, et al., 2018, 2020). Since no significant N concentrations in leaves were found at the site (Beudert and Breit, 2014), an integration of a compensation point for NO₂ is probably less useful for the measurement site. Still, further flux comparisons of oxidized nitrogen compounds to their modeled entities are needed which would possibly lead to improvements in the representation and accurate apportionment of exchange pathways in (bi)directional resistance models.

Including a soil compensation point in DEPAC, can lead to a reduction in deposition at sites with generally low ΣN_r deposition and at sites with sparse vegetation. For entire campaign, median deposition velocities for tot NH₄⁺ and tot NO₃⁻ (3.4 and 4.2 cm s⁻¹, respectively) are likewise comparable to values reported by Wolff et al. (2010). Their values for v_d agreed well with the inverse of R_{so}. Farmer et al. (2011) and Gordon et al. (2011) reported v_d for NH₄⁺ and NO₃⁻, respectively. They found an average v_d of 0.48 cm s⁻¹ for NO₃⁻ and 0.19 cm s⁻¹ for NH₄⁺ around noon.

4.2.1 Uncertainties in DEPAC-1D

Leaf area index and displacement height

Besides the current implementation of the exchange pathways in DEPAC, deposition estimates could be more accurate if concentration measurements at a higher time resolution and measurements of the LAI would have been available. We did not take measurements of the LAI or other vegetation properties at the measurement site. Still, the interpretation of differences to flux measurements would be challenging since the vegetation inside the flux footprint was not uniform. Inside the footprint, we identified dead wood in southern direction and a mix of rather young and matured trees in easterly direction. Differences in tree age were related to a dieback by bark beetle in the mid-1990s and 2000s (Beudert and Breit, 2014) from which the forest stand is still recovering. Shifting z₀ or d by ±50 %, caused a change of +5.0 %/-3.2 % and +5.6 %/-9.1 %, respectively, in the nitrogen dry deposition after 2.5 years. An incorrect assessment of the modeled LAI by ±50 % had a significant influence on the dry deposition. It led to a change of +18.9 %/-27.2 %. It shows that in further field applications of DEPAC-1D measurements the LAI should be considered, but an incorrect assessment of the LAI would not solely explain the overestimation of DEPAC-1D to TRANC measurements.

1025

Using long-term concentration averages

The main uncertainty of DEPAC-1D fluxes was most likely the usage of monthly integrated DELTA concentrations for the N_r compounds. Thus, ~~instationarities~~ the large variability in the timeseries of these compounds happened on timescales of a few seconds were not accounted in deposition modeling. Even with high-resolution measurements of the QCL, the short-term variability in NH_3 concentrations was not detectable (Wintjen et al., 2022). As stated in Sect. 2.2.3, we did not superimpose monthly concentrations values with synthetic diurnal patterns. Concentrations of N_r compounds are highly variable during the day and depend on various parameters such as turbulence, temperature, relative humidity, precipitation, and emission sources, etc. Reproducing influences of those parameters with averaged diurnal cycles about at least weeks or months, is not possible. We found that NH_3 concentration was generally low during winter and assigned with a low variability as found by measurements. During those times, using monthly integrated averages is reasonable (Schrader et al., 2018). However, we probably overestimated modeled fluxes due to the use of monthly averaged concentrations. In order to get at least an impression which N_r compounds' fluxes are probably biased by this approach, we compared monthly averaged fluxes of LOTOS-EUROS (A1) with fluxes calculated by multiplying monthly averaged v_d with their monthly concentration averages (A2) and subsequently corrected them by applying Eq. (9) and (10) of Schrader et al. (2018). Generally, we found that all N_r compounds' fluxes were overestimated by A2 whereas the difference to A1 depends on the investigated N_r compound and season. All N_r compounds had in common that the difference between both approaches was negligible during seasons with small deposition fluxes, for example in winter. Within seasons of large deposition fluxes, significant discrepancies were found, in particular for NH_3 . Overall, mean absolute deviations to A1 were 35.0, 0.27, 0.18, 0.92, 2.5, and 2.4 $ng\ N\ m^{-2}\ s^{-1}$ for NH_3 , NO_2 , NO , HNO_3 , NH_4^+ , and NO_3^- , respectively.

It should be considered that we used LOTOS-EUROS data for this comparison. Especially for NH_3 , NH_4^+ , and NO_3^- , their modeled seasonality and concentrations exhibited significant disagreements to DELTA measurements. Thus, the flux overestimations should be seen as highest guess. Measured high resolution concentrations would have led to lower values. Still, the comparison highlights the necessity for high-resolution measurements of N_r compounds. Those measurements should be made for N_r compounds, which probably prevail the exchange dynamics of ΣN_r at a certain site and thereby at least cover time periods with large temporal variations in their concentrations. This procedure was performed for NH_3 and NO_2 at the measurement site and should be considered for further measurement campaigns.

~~Devices measuring NH_3 , HNO_3 , or NO_x with a high sampling rate have high costs, high power consumption, and require regular maintenance, e.g. for NH_3 (Whitehead et al., 2008; Ferraro et al., 2012, 2021; Zöll et al., 2016; Moravek et al., 2019). A setup consisting of such instruments for each N_r compound, installed at various ecosystems is in most cases not affordable. A combination of DELTA and high-resolution sampling devices installed at sites for a limited time period to investigate concentration and flux dynamics may become a proper solution as suggested by Schrader et al. (2018) for NH_3 and could lead to significant improvements in the implemented parameterizations of various N_r compounds. Depending on vegetation and pollution climate, only high-resolution measurements of certain N_r compounds may be of interest. At agricultural sites as an example, only instruments measuring the NH_3 exchange are needed since processes controlling the ΣN_r exchange are most likely driven by a high NH_3 background concentration (Ammann et al., 2012; Brümmer et al., 2013).~~

4.3.2 Uncertainties in LOTOS-EUROS

The larger nitrogen deposition values for the measurement site as modeled by LOTOS-EUROS are mostly related to the overestimation of modeled input NH_3 concentrations. As visualized by Fig. S1, LOTOS-EUROS clearly overestimated exceed observed NH_3 concentrations in spring and autumn. Such an overestimation of NH_3 and NH_4^+ in precipitation at forest

monitoring sites was identified before for stations in Baden-Württemberg and Bavaria (Schaap et al., 2017). A similar systematic overestimation by the model in southern Germany has also been identified in comparison to novel NH₃ satellite data (Ge et al., 2020). This leads us to believe that the overestimation is for a large part due to shortcomings in the emission information (Sect. 4.1), potentially in combination with the model resolution. ~~The emission inventory used in this study spatially allocates NH₃ manure derived emissions through a procedure in which the animal numbers per region and agricultural land within a region are the two proxies used. Emissions from fertilizer application are allocated solely on land use. Hence, within a region all agricultural land is assumed to emit the same amount of NH₃, although the intensity of the agricultural practice and distribution of housing may vary substantially within such a region. Only south of the station, agricultural lands are located within 7 x 7 km² (the model resolution) of the site. This means that in the grid cell of the model, in which the station is located, there is an emission source present contributing an increased NH₃ concentration even when the wind directions are not transporting air from this agricultural region towards the station. The low measured concentrations of N_x compounds show that the site was mostly outside the transport range of nitrogen-enriched air masses.~~

A reduction in grid cell size could lead to a more precise localization of potential nitrogen emission sources and a better description of close-range transport and dilution effects. For a simulation covering 2015, we were able to calculate concentrations and fluxes at a higher grid cell resolution (2 x 2 km²) and compared the results to the standard spatial resolution (7 x 7 km²). In case of the high grid cell resolution, concentrations were lower but only by 2 to 10 % depending on the compound compared to standard spatial resolution. For the ~~whole higher~~ grid cell resolution, annual N budget ~~of the high-resolution fluxes~~ was higher than the budget of the standard spatial resolution case study, but only by 4.3 % probably due to differences in the relative fractions of land-use classes. The contribution of forest land-use classes was likely higher in case of the high spatial resolution ~~the relative increase in forest cover~~. The higher grid cell resolution probably led to improvements in modeling atmospheric turbulence resulting in higher deposition velocities. This example shows that the grid cell resolution of 7 x 7 km² is not mainly responsible for the overestimation of ~~the NH₃ concentrations and N_x fluxes~~ by LOTOS-EUROS.

Nevertheless, the seasonal cycle also indicates that the ~~emissions in spring~~ information, which LOTOS-EUROS extracts from the emission inventory, does not agree well with agricultural management practiced in the surrounding of the Bavarian Forest, ~~which are related to manure and fertilizer application, are too strong~~. The agricultural fields close to the Bavarian Forest are predominantly extensively managed grass lands. Manure application to grass lands is known to occur much more ~~spread out~~ evenly distributed across the year in comparison to the application for crop production, which mainly occurs before ~~or during~~ the growing season. Hence, in reality the emission variability maybe prone more to summer conditions ~~favoring fast mixing and dilution of NH₃~~. Currently, the detailing of crop dependent emissions made within LOTOS-EUROS, i.e. the use of variable emission fractions within German regions in combination with the recent timing module of Ge et al. (2020), is under investigation to elucidate if these factors are contributing to the ~~observed measurement-model~~ mismatches observed for the measurement site.

Additional features may also contribute to the observed differences. ~~Whitin~~ Within LOTOS-EUROS, modeled concentrations were written out for a reference height of 2.5 m above ~~z₀ ground~~, which was lower than the measurement height of the flux tower. ~~Thus, slight~~ differences between in measured and modeled micrometeorological input data ~~could be expected~~ were found, for example the difference in relative humidity in the first half of 2016. Differences for that time period were related to the usage of local meteorological data taken at 50 m, ~~which was higher than the model layer height associated with air temperature and relative humidity, with their instrumentation being installed at the 50 m platform~~. The deviations in ~~u_z u_{*}~~ as illustrated in Fig. S6 and Fig. 5 were related to differences in measurement heights at which wind speeds and roughness lengths were calculated. The model grid cell consists of various vegetation types each with a unique surface roughness length. We showed that the weighting of the land use classes within the grid cell was not in agreement with the vegetation of the flux footprint affecting micrometeorological variables, e.g. ~~u_z u_{*}~~, L , and thereby the calculation of R_a and R_b .

The large contribution of aerosols to the total deposition (Fig. 7) modeled by LOTOS-EUROS was accompanied by unusually high deposition velocities of $p\text{NH}_4^+$, $p\text{NO}_3^-$, and HNO_3 from November 2017 to February 2018. Deposition of HNO_3 and particulate nitrogen is mostly driven by the aerodynamic resistance and quasi-laminar resistance, R_a and R_b . Since v_d of those compounds was relatively high compared to measurements during that time, R_a and R_b were probably low or even close to zero. R_a and R_b depend on various parameters like u_* , the integrated stability corrections functions after Webb (1970) and Paulson (1970), surface roughness, and leaf area index. L determines the integrated stability functions and depends on wind speed close to the surface, cloud cover, and solar zenith angle (Manders-Groot et al., 2016). Snow cover is not considered in the parametrization of L yet. Including snow cover in the parametrization affect the albedo of the surface and thus the prevailing stratification of the boundary layer, which probably leads to more occurrences of stable stratification. An implementation of snow cover in the parametrization of L may reduce the deviations of simulated vs. measured stability and u_* .

~~Aerosol deposition contributed significantly to overall dry deposition of LOTOS-EUROS as shown in Fig. 7. In particular during winter, v_d of LOTOS-EUROS was greatly enhanced for NO_3^- , NH_4^+ , and HNO_3 compared to DEPAC-1D. Above snow-covered surfaces, unstable stratifications prevailed in the simulations. In addition, Figure S6 revealed large discrepancies in u_* to the measurements. Consequently, R_a and R_b were reduced compared to DEPAC-1D resulting in large deposition velocities.~~

An incorrect setting of the LAI and z_0 can have a significant influence on modeled ΣN_r deposition as shown in Sect. 4.2.1 ~~the previous chapter~~. The ~~results of our sensitivity analysis~~ relative changes in modeled ΣN_r deposition caused by ~~for~~ LAI and z_0 were comparable to values presented recently by van der Graaf et al. (2020), who used satellite-derived LAI and z_0 data from Moderate Resolution Imaging Spectroradiometer (MODIS) to calculate ΣN_r deposition with LOTOS-EUROS for a grid cell size of $7 \times 7 \text{ km}^2$. Overall, they observed changes in ΣN_r dry deposition ~~of up~~ ranging from -20 % to +30 %. However, there was almost no change in ΣN_r dry deposition and in NH_3 concentration observable for the Bavarian Forest measurement site if LAI and z_0 from MODIS were used. The attempts of van der Graaf et al. (2020) and Ge et al. (2020) did not provide a solution for the general overestimation of the NH_3 deposition above southern Germany. ~~We assume that~~ ~~It seems that larger scale and temporal~~ the spatially and temporally imprecise allocation of emission data ~~discrepancies in modeled NH_3 concentrations could be is~~ most responsible for the disagreement to flux measurements, ~~and overestimation was only partly related to other issues, for example, the grid cell size of $7 \times 7 \text{ km}^2$~~ . Further investigations on these issues are needed.

~~Summary &~~ 5. Conclusions

The annual total reactive nitrogen (ΣN_r) dry deposition estimates of all methods were in the same range considering uncertainties of measured fluxes and model applications. Annual estimates from the Total Reactive Atmospheric Nitrogen Converter (TRANC) were lower than the results from an in-situ inferential modeling approach using the bidirectional resistance scheme DEPAC (Deposition of Acidifying Compounds) (here called DEPAC-1D) and the chemical transport model LOTOS-EUROS (Long Term Ozone Simulation – EUROpean Operational Smog) v2.0. Annual dry deposition estimates of TRANC, DEPAC-1D, and LOTOS-EUROS were within the minimum and maximum dry deposition estimates of the canopy budget technique (CBT) showing ecological and micrometeorological measurements provide reasonable estimates. According to the critical load concept, annual nitrogen deposition was below critical values. Findings were supported by local vegetation samplings showing no indications for nitrogen exceedances leading to the conclusion that the critical load concept is a useful tool to describe the health status of an ecosystem. ~~We conducted a comparison of total reactive nitrogen (ΣN_r) dry deposition estimates determined by ecological and micrometeorological methods at a remote, mixed forest site for 2.5 years. We determined annual ΣN_r deposition from flux measurements by using the Total Reactive Atmospheric Nitrogen Converter (TRANC) coupled to a chemiluminescence detector (CLD), an in-situ inferential modeling approach using the bidirectional resistance scheme DEPAC (Deposition of Acidifying Compounds) (here called DEPAC-1D), the chemical transport model~~

LOTOS-EUROS (Long Term Ozone Simulation – European Operational Smog) v2.0, and by applying the canopy budget technique (CBT).

We found that modeled ΣN_r concentrations were on average at $5.0 \mu\text{g N m}^{-3}$, compared to $3.1 \mu\text{g N m}^{-3}$ measured with the TRANC for the entire campaign. A comparison to monthly integrated concentrations of compounds contributing to ΣN_r obtained from passive sampler and DELTA (DENuder of Long Term Atmospheric sampling) measurements revealed that ammonia (NH_3) concentrations were overestimated by the model by a factor of two to three compared to measured values. In addition, NH_3 contributed most to the ΣN_r concentration pattern in LOTOS-EUROS whereas NO_x was identified as predominant compound by measurements. Fluxes predicted by LOTOS-EUROS were substantially higher during spring and winter, and the diurnal flux pattern was not in agreement with TRANC fluxes. DEPAC-1D fluxes were close to the measured fluxes in winter, but deposition was clearly overestimated in summer. From May to September, TRANC and DEPAC-1D deposition velocities differed in their response to micrometeorological variables. A further investigation of stomatal vs. non-stomatal deposition pathways needs to be conducted as these are likely factors for discrepancies in modeling vs. measuring. For 2016 and 2017, the following averaged annual ΣN_r dry deposition were found:

- For TRANC measurements, 4.3 ± 0.4 and $4.7 \pm 0.2 \text{ kg N ha}^{-1} \text{ a}^{-1}$ were estimated using the Mean Diurnal Variation approach in combination with DEPAC-1D and DEPAC-1D only, respectively.
- The application of DEPAC-1D resulted in $5.8 \pm 0.1 \text{ kg N ha}^{-1} \text{ a}^{-1}$.
- For the site-specific land use fractions, $6.5 \pm 0.3 \text{ kg N ha}^{-1} \text{ a}^{-1}$ was predicted by LOTOS-EUROS
- Minimum and maximum dry deposition of the CBT analysis were 3.8 ± 0.5 and $6.7 \pm 0.3 \text{ kg N ha}^{-1} \text{ a}^{-1}$, respectively.

Including wet deposition estimates from nearby wet-only samplers in the budget calculation, resulted in annual total nitrogen depositions between 11.5 and $14.6 \text{ kg N ha}^{-1} \text{ a}^{-1}$ and between 11.7 and $14.8 \text{ kg N ha}^{-1} \text{ a}^{-1}$ for 2016 and 2017, respectively, thereby being close to the upper limit of the critical load ranges for deciduous and coniferous forests implying that the forest is just at the limit of receiving too much nitrogen from the atmosphere.

Differences between DEPAC-1D and TRANC measurements could be related to erroneous uncertainties parametrizations in parametrizing the exchange pathways of reactive gases, the usage of low-resolution input data, or the missing exchange pathway with soil. Modeled ΣN_r deposition velocities of DEPAC-1D were enhanced with regard to wet conditions, which was in contrast to TRANC measurements leading to systematically larger deposition fluxes. To a smaller extent, the same observation was made for LOTOS-EUROS, and additionally deposition velocities of DEPAC-1D and LOTOS-EUROS did not agree well in their diurnal pattern. Thus, a further investigation of stomatal vs. non-stomatal deposition pathways needs to be conducted as these are likely the main factors for discrepancies in modeled vs. measured results. Besides possible uncertainty sources in DEPAC-1D, measured dry deposition estimates using DEPAC-1D for gap-filling of both gap-filling approaches were similar showing that DEPAC-1D (and by extension, inferential modeling in general) is a valuable gap-filling tool at sites with prevailing N deposition. The difference to dry deposition estimates of LOTOS-EUROS was mainly related to an overestimation of NH_3 concentrations by a factor of two to three compared to measured concentrations. Consequently, NH_3 contributed most to the ΣN_r concentration pattern in LOTOS-EUROS whereas NO_x was identified as predominant compound by measurements. A larger scale aspect The imprecise allocation of emission data may be responsible for that issue the discrepancies to measured NH_3 concentrations since the general overestimation of NH_3 concentrations by LOTOS-EUROS has still not been solved by several attempts of model developers (van der Graaf et al., 2020; Ge et al., 2020).

We found that all estimates were in similar within reasonable margins. However, further comparisons of flux measurements and model applications are needed to investigate exchange characteristics of ΣN_r and its individual compounds, if possible, simultaneously and at different ecosystems. Measuring several N_r compounds and ΣN_r at a high time resolution is probably not affordable due to operating and maintenance costs, high technical requirements, and time-consuming processing of the acquired data. A solution could be continuous monitoring of N_r compounds by low-cost samplers complemented by high-

1195 frequency measurements of ΣN_r and selected compounds like NH_3 for a limited time, which will result in a better understanding
of exchange processes and thus in an improvement of deposition models (cf. Schrader et al., 2020~~18~~).

1200 *Code and data availability.* All data are available upon request from the first author of this study (pascal.wintjen@thuenen.de).
Concentration, flux, and micrometeorological data from measurements and ecological information about the site are included
in the following repository: <https://zenodo.org/record/5841074> (Brümmer et al., 2022a). Also, Python 3.7 code for flux data
analysis can be requested from the first author.

1205

Author contributions. PW, FS, MS, and CB conceived the study. PW wrote the manuscript, carried out the measurements at
the forest site, and the comparison of measured and modeled flux data and interpretation. FS evaluated meteorological
measurements and set up DEPAC-1D. MS and RK provided insights in interpreting LOTOS-EUROS results. BB conducted
1210 canopy throughfall and wet deposition measurements. CB installed the instruments at the site. The results were thoroughly
discussed with all authors, and FS, MS, BB, RK, and CB contributed to the manuscript.

1215 *Competing interests.* The authors declare that they have no conflict of interest.

Acknowledgements. We thank Undine Zöll for scientific and logistical help to the measurements, Jeremy Rüffer and Jean-
1220 Pierre Delorme for excellent technical support, Ute Tambor, Andrea Niemeyer, and Dr. Daniel Ziehe for conducting laboratory
analyses of denuder and filter samples, and the Bavarian Forest Nationalpark (NPBW) Administration, namely Wilhelm Breit
and Ludwig Höcker for technical and logistical support at the measurement site.

1225 *Financial support.* This work has been funded by the German Environment Agency (UBA) (project FORESTFLUX, support
code FKZ 3715512110) and by the German Federal Ministry of Education and Research (BMBF) within the framework of the
Junior Research Group NITROSPHERE (support code FKZ 01LN1308A).

References

- Ahrends, B., Schmitz, A., Prescher, A.-K., Wehberg, J., Geupel, M., Henning, A., and Meesenburg, H.: Comparison of
1230 Methods for the Estimation of Total Inorganic Nitrogen Deposition to Forests in Germany, *Frontiers in Forests and Global
Change*, 3, 1–22, doi: 10.3389/ffgc.2020.00103, 2020.
- Ammann, C., Wolff, V., Marx, O., Brümmer, C., and Neftel, A.: Measuring the biosphere-atmosphere exchange of total
reactive nitrogen by eddy covariance, *Biogeosciences*, 9, 4247–4261, doi: 10.5194/bg-9-4247-2012, 2012.

- Ammann, C., Jocher M., and Voglmeier, K.: Eddy Covariance Flux Measurements of NH₃ and NO_y with a Dual-Channel Thermal Converter," *IEEE International Workshop on Metrology for Agriculture and Forestry (MetroAgriFor)*, pp. 46-51, doi: 10.1109/MetroAgriFor.2019.8909278, 2019.
- 1235 Barr, A., Richardson, A., Hollinger, D., Papale, D., Arain, M., Black, T., Bohrer, G., Dragoni, D., Fischer, M., Gu, L., Law, B., Margolis, H., McCaughey, J., Munger, J., Oechel, W., and Schaeffer, K.: Use of change-point detection for friction-velocity threshold evaluation in eddy covariance studies, *Agricultural and Forest Meteorology*, 171–172, 31–45, doi: 10.1016/j.agrformet.2012.11.023, 2013.
- 1240 ~~Beudert, B. and Breit, W.: Integrated Monitoring Programm an der Meßstelle Forellenbach im Nationalpark Bayerischer Wald, Untersuchungen zum Stickstoffeintrag und zum wassergebundenen Stickstoffhaushalt des Forellenbachgebiets, Förderkennzeichen 351 01 012. Nationalparkverwaltung Bayerischer Wald, Sachgebiet IV, techreport, Umweltbundesamt, Dessau-Roßlau, Germany, available at: http://www.umweltbundesamt.de/sites/default/files/medien/370/dokumente/ece_im_forellenbach_berichtsjahr_2009.pdf (last access: 14 March 2022), 2010.~~
- 1245 Beudert, B. and Breit, W.: Kronenraumbilanzen zur Abschätzung der Stickstoffgesamtdosition in Waldökosysteme des Nationalparks Bayerischer Wald, techreport, Umweltbundesamt, Dessau-Roßlau, Germany, available at: https://www.umweltbundesamt.de/sites/default/files/medien/370/dokumente/kronenraumbilanzen_stickstoffgesamtdosition_nationalpark_bayerisches_wald_-_berichtsjahr_2013_im_forellenbach.pdf (last access: 14 March 2022), 2014.
- 1250 ~~Beudert, B., and Gietl, G.: Long term monitoring in the Große Ohe catchment, Bavarian Forest National Park, Silva Gabreta, 21, 5–27, https://www.npsumava.cz/wp-content/uploads/2019/06/sg_21_1_beudertgietl.pdf (last access: 14 March 2022), 2015.~~
- Bobbink, R., Hornung, M. and Roelofs, J. G. M.: The effects of air-borne nitrogen pollutants on species diversity in natural and semi-natural European vegetation, *Journal of Ecology*, 86, 717–738, doi:10.1046/j.1365-2745.1998.8650717.x, 1998.
- 1255 Bobbink, R. and Hettelingh, J.-P.: Review and revision of empirical critical loads and dose-response relationships. National Institute for Public Health and the Environment (RIVM), RIVM Report, <https://www.rivm.nl/bibliotheek/rapporten/680359002.pdf> (last access: 14 March 2022), 2011.
- Breuninger, C., Meixner, F. X., and Kesselmeier, J.: Field investigations of nitrogen dioxide (NO₂) exchange between plants and the atmosphere, *Atmospheric Chemistry and Physics*, 13, 773–790, doi:10.5194/acp-13-773-2013, 2013.
- 1260 Brümmer, C., Marx, O., Kutsch, W., Ammann, C., Wolff, V., Flechard, C. R., and Freibauer, A.: Fluxes of total reactive atmospheric nitrogen (ΣN_r) using eddy covariance above arable land, *Tellus B: Chemical and Physical Meteorology*, 65, 19770, doi:10.3402/tellusb.v65i0.19770, 2013.
- Brümmer, C., Ruffer, J. J., Delorme, J.-P., Wintjen, P., Schrader, F., Beudert, B., Schaap, M., and Ammann, C.: Reactive nitrogen fluxes over peatland and forest ecosystems using micrometeorological measurement techniques, *Earth System Science Data*, 14, 743-761, doi:10.5194/essd-14-743-2022, 2022.
- 1265 Brümmer, C., Ruffer, J. J., Delorme, J.-P., Wintjen, P., Schrader, F., Beudert, B., Schaap, M., and Ammann, C.: Reactive nitrogen fluxes over peatland (Bourtanger Moor) and forest (Bavarian Forest National Park) using micrometeorological measurement techniques (1.1) [Data set]. Zenodo. doi:10.5281/zenodo.5841074, 2022a.
- 1270 Butterbach-Bahl, K., Gasche, R., Breuer, L., and Papen, H.: Fluxes of NO and N₂O from temperate forest soils: impact of forest type, N deposition and of liming on the NO and N₂O emissions, *Nutrient Cycling in Agroecosystems*, 48, 79–90, doi:10.1023/a:1009785521107, 1997.
- Chaparro-Suarez, I., Meixner, F., and Kesselmeier, J.: Nitrogen dioxide (NO₂) uptake by vegetation controlled by atmospheric concentrations and plant stomatal aperture, *Atmospheric Environment*, 45, 5742–5750, doi:10.1016/j.atmosenv.2011.07.021, 2011
- 1275

- Damgaard, C., Jensen, L., Frohn, L. M., Borchsenius, F., Nielsen, K. E., Ejrnæs, R. and Stevens, C. J.: The effect of nitrogen deposition on the species richness of acid grasslands in Denmark: A comparison with a study performed on a European scale, *Environmental Pollution*, 159, 1778-1782, doi:10.1016/j.envpol.2011.04.003, 2011.
- 1280 Delaria, E. R., Vieira, M., Cremieux, J., and Cohen, R. C.: Measurements of NO and NO₂ exchange between the atmosphere and *Quercus agrifolia*, *Atmospheric Chemistry and Physics*, 18, 14 161–14 173, doi:10.5194/acp-18-14161-2018, 2018.
- Delaria, E. R., Place, B. K., Liu, A. X., and Cohen, R. C.: Laboratory measurements of stomatal NO₂ deposition to native California trees and the role of forests in the NO_x cycle, *Atmospheric Chemistry and Physics*, 20, 14 023–14 041, doi:10.5194/acp-20-14023-2020, 2020.
- 1285 de Vries, W., Reinds, G. J., and Vel, E.: Intensive monitoring of forest ecosystems in Europe: 2: Atmospheric deposition and its impacts on soil solution chemistry, *Forest Ecology and Management*, 174, 97–115, doi:10.1016/S0378-1127(02)00030-0, 2003.
- Dimböck, T., Grandin, U., Bernhardt-Römermann, M., Beudert, B., Canullo, R., Forsius, M., Grabner, M.-T., Holmberg, M., Kleemola, S., Lundin, L., Mirtl, M., Neumann, M., Pompei, E., Salemaa, M., Starlinger, F., Staszewski, T., and Uziębło, A. K.: Forest floor vegetation response to nitrogen deposition in Europe, *Global Change Biology*, 20, 429-440, doi:10.1111/gcb.12440, 2014.
- 1290 Dimböck, T., Pröll, G., Austnes, K., Beloica, J., Beudert, B., Canullo, R., De Marco, A., Fornasier, M. F., Futter, M., Goergen, K., Grandin, U., Holmberg, M., Lindroos, A.-J., Mirtl, M., Neiryneck, J., Pecka, T., Nieminen, T. M., Nordbakken, J.-F., Posch, M., Reinds, G.-J., Rowe, E. C., Salemaa, M., Scheuschner, T., Starlinger, F., Uziębło, A. K., Valinia, S., Weldon, J., Wamelink, W. G. W., and Forsius, M.: Currently legislated decreases in nitrogen deposition will yield only limited plant species recovery in European forests, *Environmental research letters*, 13, 125010, doi:10.1088/1748-9326/aaf26b, 2018.
- 1295 Draaijers, G. P. J. and Erisman, J. W.: A canopy budget model to assess atmospheric deposition from throughfall measurements, *Water, Air, Soil Pollution*, 85, 2253–2258, doi:10.1007/BF01186169, 1995.
- Emberson, L. D., Ashmore, M. R., Simpson, D., Tuovinen, J.-P. and Cambridge, H. M.: Towards a model of ozone deposition and stomatal uptake over Europe, EMEP/MS-CW 6/2000, Norwegian Meteorological Institute, Oslo, 2000a.
- 1300 Emberson, L. D., Ashmore, M. R., Cambridge, H. M., Simpson, D., and Tuovinen, J. P.: Modelling stomatal ozone flux across Europe, *Environmental Pollution*, 109, 403–413, doi:10.1016/S0269-7491(00)00043-9, 2000b.
- Erisman, J. W., Van Pul, A., and Wyers, P.: Parametrization of surface resistance for the quantification of atmospheric deposition of acidifying pollutants and ozone, *Atmospheric Environment*, 28, 2595–2607, doi:10.1016/1352-2310(94)90433-2, 1994.
- 1305 Erisman, J. W., Galloway, J., Seitzinger, S., Bleeker, A. and Butterbach-Bahl, K.: Reactive nitrogen in the environment and its effect on climate change, *Current Opinion in Environmental Sustainability*, 3, 281-290, doi:10.1016/j.cosust.2011.08.012, 2011.
- Erisman, J. W., Galloway, J. N., Seitzinger, S., Bleeker, A., Dise, N. B., Petrescu, A. M., Leach, A. M. and de Vries, W.: Consequences of human modification of the global nitrogen cycle, *Philosophical Transactions of the Royal Society London B: Biological Sciences*, 368, 201301116, doi:10.1098/rstb.2013.0116, 2013.
- 1310 Falge, E., Baldocchi, D., Olson, R., Anthoni, P., Aubinet, M., Bernhofer, C., Burba, G., Ceulemans, R., Clement, R., Dolman, H., Granier, A., Gross, P., Grünwald, T., Hollinger, D., Jensen, N.-O., Katul, G., Keronen, P., Kowalski, A., Lai, C. T., Law, B. E., Meyers, T., Moncrieff, J., Moors, E., Munger, J., Pilegaard, K., Üllar Rannik, Rebmann, C., Suyker, A., Tenhunen, J., Tu, K., Verma, S., Vesala, T., Wilson, K., and Wofsy, S.: Gap filling strategies for defensible annual sums of net ecosystem exchange, *Agricultural and Forest Meteorology*, 107, 43–69, doi:10.1016/S0168-1923(00)00225-2, 2001.
- 1315 Farmer, D. K., Wooldridge, P. J., and Cohen, R. C.: Application of thermal-dissociation laser induced fluorescence (TD-LIF) to measurement of HNO₃, Σalkyl nitrates, Σperoxy nitrates, and NO₂ fluxes using eddy covariance, *Atmospheric Chemistry and Physics*, 6, 3471–3486, doi:10.5194/acp-6-3471-2006, 2006.

- Farmer, D. K. and Cohen, R. C.: Observations of HNO₃, ΣAN, ΣPN and NO₂ fluxes: evidence for rapid HO_x chemistry within a pine forest canopy, *Atmospheric Chemistry and Physics*, 8, 3899–3917, doi:10.5194/acp-8-3899-2008, 2008.
- ~~Farmer, D. K., Kimmel, J. R., Phillips, G., Docherty, K. S., Worsnop, D. R., Sueper, D., Nemitz, E., and Jimenez, J. L.: Eddy covariance measurements with high-resolution time-of-flight aerosol mass spectrometry: a new approach to chemically resolved aerosol fluxes, *Atmos. Meas. Tech.*, 4, 1275–1289, doi:10.5194/amt-4-1275-2011, 2011.~~
- ~~Farmer, D. K., Chen, Q., Kimmel, J. R., Docherty, K. S., Nemitz, E., Artaxo, P. A., Cappa, C. D., Martin, S. T., and Jimenez, J. L.: Chemically Resolved Particle Fluxes Over Tropical and Temperate Forests, *Aerosol Science and Technology*, 47:7, 818–830, doi:10.1080/02786826.2013.791022, 2013.~~
- Ferm, M.: A Sensitive Diffusional Sampler, Report L91-172, Swedish Environmental Research Institute, Gothenburg, 1991.
- Ferrara, R. M., Loubet, B., Di Tommassi, P., Bertolini, T., Magliulo, V., Cellier, P., Eugster, W., and Rana, G.: Eddy covariance measurement of ammonia fluxes: Comparison of high frequency correction methodologies, *Agricultural and Forest Meteorology*, 158-159, 30-42, doi:10.1016/j.agrformet.2012.02.001, 2012.
- Ferrara, R. M., Di Tommassi, P., Farmulari, D., and Rana G.: Limitations of an Eddy-Covariance System in Measuring Low Ammonia Fluxes, *Boundary-Layer Meteorology*, 180, 173-186, doi:10.1007/s10546-021-00612-6, 2021.
- Finkelstein, P. L. and Sims, P. F.: Sampling error in eddy correlation flux measurements, *Journal of Geophysical Research: Atmospheres*, 106, 3503–3509, doi: 10.1029/2000JD900731, 2001.
- Flechard, C. R., Nemitz, E., Smith, R. I., Fowler, D., Vermeulen, A. T., Bleeker, A., Erismann, J. W., Simpson, D., Zhang, L., Tang, Y. S., and Sutton, M. A.: Dry deposition of reactive nitrogen to European ecosystems: a comparison of inferential models across the NitroEurope network, *Atmos. Chem. Phys.*, 11, 2703–2728, doi:10.5194/acp-11-2703-2011, 2011.
- Flechard, C. R., Ibrom, A., Skiba, U. M., de Vries, W., van Oijen, M., Cameron, D. R., Dise, N. B., Korhonen, J. F. J., Buchmann, N., Legout, A., Simpson, D., Sanz, M. J., Aubinet, M., Loustau, D., Montagnani, L., Neiryneck, J., Janssens, I. A., Pihlatie, M., Kiese, R., Siemens, J., Francez, A.-J., Augustin, J., Varlagin, A., Olejnik, J., Juszczak, R., Aurela, M., Berveiller, D., Chojnicki, B. H., Dammgen, U., Delapierre, N., Djuricic, V., Drewer, J., Dufrene, E., Eugster, W., Fauvel, Y., Fowler, D., Frumau, A., Granier, A., Gross, P., Hamon, Y., Helfter, C., Hensen, A., Horvath, L., Kitzler, B., Kruijt, B., Kutsch, W. L., Lobo-do Vale, R., Lohila, A., Longdoz, B., Marek, M. V., Matteucci, G., Mitosinkova, M., Moreaux, V., Neftel, A., Ourcival, J.-M., Pilegaard, K., Pita, G., Sanz, F., Schjoerring, J. K., Sebastia, M.-T., Tang, Y. S., Uggerud, H., Urbaniak, M., van Dijk, N., Vesala, T., Vidic, S., Vincke, C., Weidinger, T., Zechmeister-Boltenstern, S., Butterbach-Bahl, K., Nemitz, E., and Sutton, M. A.: Carbon–nitrogen interactions in European forests and semi-natural vegetation – Part 1: Fluxes and budgets of carbon, nitrogen and greenhouse gases from ecosystem monitoring and modelling, *Biogeosciences*, 17, 1583–1620, doi:10.5194/bg-17-1583-2020, 2020.
- Fowler, D., Coyle, M., Skiba, U., Sutton, M. A., Cape, J. N., Reis, S., Sheppard, L. J., Jenkins, A., Grizzetti, B., Galloway, J. N., Vitousek, P., Leach, A., Bouwman, A. F., Butterbach-Bahl, K., Dentener, F., Stevenson, D., Amann, M. and Voss, M.: The global nitrogen cycle in the twenty-first century, *Philosophical Transactions of the Royal Society B: Biological Sciences*, 368, 20130164, doi: 10.1098/rstb.2013.0164, 2013.
- Galloway, J. N., Aber, J. D., Erismann, J. W., Seitzinger, S. P., Howarth, R. W., Cowling, E. B. and Cosby, B. J.: The Nitrogen Cascade, *BioScience*, 53, 341-356, doi: 10.1641/0006-3568(2003)053[0341:TNC]2.0.CO;2, 2003.
- Garland, J. A.: The Dry Deposition of Sulphur Dioxide to Land and Water Surfaces, *Proceedings of the Royal Society A: Mathematical, Physical and Engineering Sciences*, 354, 245–268, doi:10.1098/rspa.1977.0066, 1977.
- Ge, X., Schaap, M., Kranenburg, R., Segers, A., Reinds, G. J., Kros, H., and de Vries, W.: Modeling atmospheric ammonia using agricultural emissions with improved spatial variability and temporal dynamics, *Atmos. Chem. Phys.*, 20, 16055–16087, doi:10.5194/acp-20-16055-2020, 2020.

- 1360 Geddes, J. A. and Murphy, J. G.: Observations of reactive nitrogen oxide fluxes by eddy covariance above two midlatitude North American mixed hardwood forests, *Atmospheric Chemistry and Physics*, 14, 2939–2957, doi:10.5194/acp-14-2939-2014, 2014.
- ~~Gordon, M., Staebler, R. M., Liggio, J., Vlasenko, A., Li, S. M., and Hayden, K.: Aerosol flux measurements above a mixed forest at Borden, Ontario, *Atmos. Chem. Phys.*, 11, 6773–6786, doi:10.5194/acp-11-6773-2011, 2011.~~
- 1365 Grandin, U.: Epiphytic algae and lichen cover in boreal forests - a long-term study along a N and S deposition gradient in Sweden, *Ambio*, 40, 8, 857–866, doi: 10.1007/s13280-011-0205-x, 2011.
- Hansen, K., Sørensen, L. L., Hertel, O., Geels, C., Skjøth, C. A., Jensen, B., and Boegh, E.: Ammonia emissions from deciduous forest after leaf fall, *Biogeosciences*, 10, 4577–4589, doi:10.5194/bg-10-4577-2013, 2013.
- Hansen, K., Pryor, S. C., Boegh, E., Hornsby, K. E., Jensen, B., and Sørensen, L. L.: Background concentrations and fluxes of atmospheric ammonia over a deciduous forest, *Agricultural and Forest Meteorology*, 214–215, 380–392, doi:10.1016/j.agrformet.2015.09.004, 2015.
- 1370 Hettelingh, J.-P., Posch, M., De Smet, P. A. M. and Downing, R. J.: The use of critical loads in emission reduction agreements in Europe, *Water, Air, and Soil Pollution.*, 85, 2381–2385, doi:10.1007/BF01186190, 1995.
- Hettelingh, J.-P., Posch, M., Velders, G. J. M., Ruysenaars, P., Adams, M., de Leeuw, F., Lükewille, A., Maas, R., Sliggers, J. and Slootweg, J.: Assessing interim objectives for acidification, eutrophication and ground-level ozone of the EU National Emission Ceilings Directive with 2001 and 2012 knowledge, *Atmospheric Environment*, 75, 129–140, doi:10.1016/j.atmosenv.2013.03.060, 2013.
- Horii, C. V., Munger, J. W., Wofsy, S. C., Zahniser, M., Nelson, D., and McManus, J. B.: Fluxes of nitrogen oxides over a temperate deciduous forest, *Journal of Geophysical Research: Atmospheres*, 109, doi:10.1029/2003JD004326, 2004.
- 1380 Horii, C. V., Munger, J. W., Wofsy, S. C., Zahniser, M., Nelson, D., and McManus, J. B.: Atmospheric reactive nitrogen concentration and flux budgets at a Northeastern US forest site, *Agricultural and Forest Meteorology*, 136, 159–174, doi:10.1016/j.agrformet.2006.03.005, 2006.
- Jarvis, P. G.: The Interpretation of the Variations in Leaf Water Potential and Stomatal Conductance Found in Canopies in the Field, *Philos. T. R. Soc. B*, 273, 593–610, doi:10.1098/rstb.1976.0035, 1976.
- 1385 Jensen, N. and Hummelshøj, P.: Derivation of canopy resistance for water vapor fluxes over a spruce forest, using a new technique for the viscous sublayer resistance (correction to vol. 73, p. 339, 1995), *Agricultural and Forest Meteorology*, 85, 289, doi:10.1016/S0168-1923(97)00024-5, 1997.
- Jensen, N. O. and Hummelshøj, P.: Derivation of canopy resistance for water-vapor fluxes over a spruce forest, using a new technique for the viscous sublayer resistance, *Agricultural and Forest Meteorology*, 73, 339–352, doi:10.1016/0168-1923(94)05083-I, 1995.
- 1390 Jung, H., Senf, C., Beudert, B., and Krueger, T.: Bayesian hierarchical modeling of nitrate concentration in a forest stream affected by large-scale forest dieback, *Water Resources Research*, 57, 2, e2020WR027264, doi: 10.1029/2020WR027264 2021.
- Krupa, S. V.: Effects of atmospheric ammonia (NH₃) on terrestrial vegetation: a review, *Environmental Pollution*, 124, 179–211, doi: 10.1016/S0269-7491(02)00434-7, 2003.
- 1395 Kuenen, J., Dellaert, S., Visschedijk, A., Jalkanen, J.-P., Super, I., and Denier van der Gon, H.: CAMS-REG-v4: a state-of-the-art high-resolution European emission inventory for air quality modelling, *Earth System Science Data*, 14, 491–515, doi: 10.5194/essd-14-491-2022, 2022. ~~Earth Syst. Sci. Data Discuss. [preprint], doi:10.5194/essd-2021-242, in review, 2021~~
- Kundu, S., Kawamura, K., and Lee, M.: Seasonal variation of the concentrations of nitrogenous species and their nitrogen isotopic ratios in aerosols at Gosan, Jeju Island: Implications for atmospheric processing and source changes of aerosols, *Journal of Geophysical Research: Atmospheres.*, 115, D20305, doi: 10.1029/2009JD013323, 2010.
- 1400

- Li, Y., Schichtel, B. A., Walker, J. T., Schwede, D. B., Chen, X., Lehman, C. M. B., Puchalski, M. A., Gay, D. A., and Collett, J. L.: Increasing importance of deposition of reduced nitrogen in the United States, *Proceedings of the National Academy of Sciences*, 113, 5874–5879, doi: 10.1073/pnas.1525736113, 2016.
- 1405 ~~LTFR: Long Term Ecological Research (LTFR) network, available at: <https://deims.org/993ed2fe-1eb0-4810-a619-8bef78b6eccc> (last access: 14 March 2022), 2022.~~
- Marx, O., Brümmner, C., Ammann, C., Wolff, V., and Freibauer, A.: TRANC – a novel fast-response converter to measure total reactive atmospheric nitrogen, *Atmospheric Measurement Techniques*, 5, 1045–1057, doi:10.5194/amt-5-1045-2012, 2012.
- 1410 Manders-Groot, A. M. M., Segers, A. J., and Jonkers, S.: LOTOS-EUROS v2.0 Reference Guide, TNO report TNO2016 R10898, TNO, Utrecht, The Netherlands, https://lotos-euros.tno.nl/media/10360/reference_guide_v2-0_r10898.pdf (last access: 14 March 2022), 2016.
- Manders, A. M. M., Builtjes, P. J. H., Curier, L., Denier van der Gon, H. A. C., Hendriks, C., Jonkers, S., Kranenburg, R., Kuenen, J. J. P., Segers, A. J., Timmermans, R. M. A., Visschedijk, A. J. H., Wichink Kruit, R. J., van Pul, W. A. J., Sauter, F.
- 1415 J., van der Swaluw, E., Swart, D. P. J., Douros, J., Eskes, H., van Meijgaard, E., van Ulft, B., van Velthoven, P., Banzhaf, S., Mues, A. C., Stern, R., Fu, G., Lu, S., Heemink, A., van Velzen, N., and Schaap, M.: Curriculum vitae of the LOTOS–EUROS (v2.0) chemistry transport model, *Geoscientific Model Development*, 10, 4145–4173, doi:10.5194/gmd-10-4145-2017, 2017.
- Milford, C., Hargreaves, K. J., Sutton, M. A., Loubet, B., and Cellier, P.: Fluxes of NH₃ and CO₂ over upland moorland in the vicinity of a agricultural land, *Journal of Geophysical Research: Atmospheres*, 106, 24 169–24 181, doi:10.1029/2001jd900082,
- 1420 2001.
- Min, K.-E., Pusede, S. E., Browne, E. C., LaFranchi, B. W., Wooldridge, P. J., and Cohen, R. C.: Eddy covariance fluxes and vertical concentration gradient measurements of NO and NO₂ over a ponderosa pine ecosystem: observational evidence for within canopy chemical removal of NO_x, *Atmospheric Chemistry and Physics*, 14, 5495–5512, doi:10.5194/acp-14-5495-2014, 2014.
- 1425 Moravek, A., Singh, S., Pattey, E., Pelletier, L., and Murphy, J. G.: Measurements and quality control of ammonia eddy covariance fluxes: A new strategy for high frequency attenuation correction, *Atmospheric Measurement Techniques*, 12, 6059–6078, doi:10.5194/amt-12-6059-2019, 2019.
- Munger, J. W., Wofsy, S. C., Bakwin, P. S., Fan, S. M., Goulden, M. L., Daube, B. C., Goldstein, A. H., Moore, K. E., and Fitzjarrald, D. R.: Atmospheric deposition of reactive nitrogen oxides and ozone in a temperate deciduous forest and a subarctic
- 1430 woodland: 1. Measurements and mechanisms, *Journal of Geophysical Research-Atmospheres*, 101, 12 639–12 657, doi:10.1029/96JD00230, 1996.
- Nemitz, E., Sutton, M. A., Wyers, G. P., and Jongejan, P. A. C.: Gas-particle interactions above a Dutch heathland: I. Surface exchange fluxes of NH₃, SO₂, HNO₃ and HCl, *Atmospheric Chemistry and Physics*, 4, 989–1005, doi:10.5194/acp-4-989-2004, 2004.
- 1435 Paulissen, M.P.C.P., Bobbink, R., Robat, S.A., and Verhoeven, J. T. A.: Effects of Reduced and Oxidised Nitrogen on Rich-Fen Mosses: a 4-Year Field Experiment., *Water, Air, & Soil Pollution*, 227, 18, doi:10.1007/s11270-015-2713-y, 2016.
- Paulson, C. A.: The Mathematical Representation of Wind Speed and Temperature Profiles in the Unstable Atmospheric Surface Layer, *Journal of Applied Meteorology*, 9, 857–861, doi:10.1175/1520-0450(1970)009<0857:Tmrows>2.0.Co;2, 1970.
- 1440 ~~Pryor, S. C., Barthelmie, R. J., Sørensen, L. L., and Jensen, B.: Ammonia concentrations and fluxes over a forest in the midwestern USA, *Atmospheric Environment*, 35, 5645–5656, doi:10.1016/S1352-2310(01)00259-X, 2001.~~
- ~~Pryor, S. and Klemm, O.: Experimentally derived estimates of nitric acid dry deposition velocity and viscous sub-layer resistance at a conifer forest, *Atmospheric Environment*, 38, 2769–2777, doi:10.1016/j.atmosenv.2004.02.038, 2004.~~

- Reichstein, M., Falge, E., Baldocchi, D., Papale, D., Aubinet, M., Berbigier, P., Bernhofer, C., Buchmann, N., Gilmanov, T.,
 1445 Granier, A., Grünwald, T., Havránková, K., Ilvesniemi, H., Janous, D., Knohl, A., Laurila, T., Lohila, A., Loustau, D.,
 Matteucci, G., Meyers, T., Miglietta, F., Ourcival, J.-M., Pumpanen, J., Rambal, S., Rotenberg, E., Sanz, M., Tenhunen, J.,
 Seufert, G., Vaccari, F., Vesala, T., Yakir, D., and Valentini, R.: On the separation of net ecosystem exchange into assimilation
 and ecosystem respiration: review and improved algorithm, *Global Change Biology*, 11, 1424–1439, doi:10.1111/j.1365-
 2486.2005.001002.x, 2005.
- 1450 Putaud, J.-P., Van Dingenen, R., Alastuey, A., Bauer, H., Birmili, W., Cyrys, J., Flentje, H., Fuzzi, S., Gehrig, R., Hansson,
 H., Harrison, R., Herrmann, H., Hitzenberger, R., Hüglin, C., Jones, A., Kasper-Giebl, A., Kiss, G., Kousa, A., Kuhlbusch, T.,
 Löschau, G., Maenhaut, W., Molnar, A., Moreno, T., Pekkanen, J., Perrino, C., Pitz, M., Puxbaum, H., Querol, X., Rodriguez,
 S., Salma, I., Schwarz, J., Smolik, J., Schneider, J., Spindler, G., ten Brink, H., Tursic, J., Viana, M., Wiedensohler, A., and
 Raes, F.: A European aerosol phenomenology – 3: Physical and chemical characteristics of particulate matter from 60 rural,
 1455 urban, and kerbside sites across Europe, *Atmospheric Environment*, 44, 1308–1320, doi: 10.1016/j.atmosenv.2009.12.011,
 2010.
- ~~Rondon, A., Johansson, C., and Granat, L.: Dry Deposition of Nitrogen Dioxide and Ozone to Coniferous Forests, *Journal of
 Geophysical Research-Atmospheres*, 98, 5159–5172, doi:10.1029/92jd02335, 1993.~~
- Rosenkranz, P., Brüggemann, N., Papen, H., Xu, Z., Seufert, G., and Butterbach-Bahl, K.: N₂O, NO and CH₄ exchange, and
 1460 microbial N turnover over a Mediterranean pine forest soil, *Biogeosciences*, 3, 121–133, doi:10.5194/bg-3-121-2006, 2006.
- Roth, M., Müller-Meißner, A., Michiels, H.-G., and Hauck, M.: Vegetation changes in the understory of nitrogen-sensitive
 temperate forests over the past 70 years, *Forest Ecology and Management*, 503, 119754, doi:10.1016/j.foreco.2021.119754
 2022.
- Rummel, U., Ammann, C., Gut, A., Meixner, F. X., and Andreae, M. O.: Eddy covariance measurements of nitric oxide flux
 1465 within an Amazonian rain forest, *Journal of Geophysical Research-Atmospheres*, 107, LBA 17–1–LBA 17–9,
 doi:10.1029/2001JD000520, 2002.
- Sauter, F., Sterk, M., van der Swaluw, E., Wichink Kruit, R., de Vries, W., and van Pul, A.: The OPS-model: Description of
 OPS 5.0.0.0, RIVM, Bilthoven, <https://www.rivm.nl/media/ops/OPS-model.pdf> (last access: 14 March 2022), 2020.
- Saylor, R. D., Baker, B. D., Lee, P., Tong, D., Pan, L., and Hicks, B. B.: The particle dry deposition component of total
 1470 deposition from air quality models: right, wrong or uncertain?, *Tellus B: Chemical and Physical Meteorology*, 71, 1550324,
 doi: 10.1080/16000889.2018.1550324, 2019.
- Schaap, M., Wichink Kruit, R., Hendriks, C., Kranenburg, R., Segers, A., Bultjes, P., and Banzhaf, S.: Modelling and
 an assessment of acidifying and eutrophying atmospheric deposition to terrestrial ecosystems (PINETI-2): Part I: Atmospheric
 deposition to German natural and semi-natural ecosystems during 2009, 2010 and 2011, technical report, Umweltbundesamt,
 1475 Dessau-Roßlau, Germany, [https://www.umweltbundesamt.de/sites/default/files/medien/1410/publikationen/2017-08-
 15_texte_62-2017_pineti2-teil1.pdf](https://www.umweltbundesamt.de/sites/default/files/medien/1410/publikationen/2017-08-15_texte_62-2017_pineti2-teil1.pdf) (last access: 14 March 2022), 2017.
- Schaap, M., Hendriks, C., Kranenburg, R., Kuenen, J., Segers, A., Schlutow, A., Nagel, H.-D., Ritter, A., and Banzhaf, S.:
 PINETI-3: Modellierung atmosphärischer Stoffeinträge von 2000 bis 2015 zur Bewertung der ökosystem-spezifischen
 Gefährdung von Biodiversität durch Luftschadstoffe in Deutschland, technical report, Umweltbundesamt, Dessau-Roßlau,
 1480 Germany, [https://www.umweltbundesamt.de/sites/default/files/medien/1410/publikationen/2018-10-17_texte_79-
 2018_pineti3.pdf](https://www.umweltbundesamt.de/sites/default/files/medien/1410/publikationen/2018-10-17_texte_79-2018_pineti3.pdf) (last access: 14 March 2022), 2018.
- Schneider, C., Pelzer, M., Toenges-Schuller, N., Nacken, M., & Niederau, A.: ArcGIS basierte Lösung zur detaillierten,
 deutschlandweiten Verteilung (Gridding) nationaler Emissionsjahreswerte auf Basis des Inventars zur
 Emissionsberichterstattung - Kurzfassung; UBA TEXTE 71/2016. Für Mensch & Umwelt,
 1485 <https://www.umweltbundesamt.de/publikationen/arcgis-basierte-loesung-zur-detaillierten> (last access: 9 June 2022), 2016.

- Schrader, F. and Brümmner, C.: Land Use Specific Ammonia Deposition Velocities: a Review of Recent Studies (2004–2013), *Water, Air, and Soil Pollution*, 225, 2114, doi:10.1007/s11270-014-2114-7, 2014.
- Schrader, F., Brümmner, C., Flechard, C. R., Wichink Kruit, R. J., van Zanten, M. C., Zöll, U., Hensen, A., and Erisman, J. W.: Non-stomatal exchange in ammonia dry deposition models: comparison of two state-of-the-art approaches, *Atmospheric Chemistry and Physics*, 16, 13417–13430, doi:10.5194/acp-16-13417-2016, 2016.
- 1490 Schrader, F., Schaap, M., Zöll, U., Kranenburg, R., and Brümmner, C.: The hidden cost of using low-resolution concentration data in the estimation of NH₃ dry deposition fluxes, *Scientific Reports*, 8, 969, doi:10.1038/s41598-017-18021-6, 2018.
- Schrader, F., Erisman, J. W., and Brümmner, C.: Towards a coupled paradigm of NH₃-CO₂ biosphere-atmosphere exchange modelling. *Global Change Biology*, 26, 4654–4663, doi: 10.1111/gcb.15184, 2020.
- 1495 Schwarz, J., Cusack, M., Karban, J., Chalupníčková, E., Havránek, V., Smolík, J., and Ždímal, V.: PM_{2.5} chemical composition at a rural background site in Central Europe, including correlation and air mass back trajectory analysis, *Atmospheric Research*, 176–177, 108–120, doi: 10.1016/j.atmosres.2016.02.017, 2016.
- Schwede, D., Zhang, L., Vet, R., and Lear, G.: An intercomparison of the deposition models used in the CASTNET and CAPMoN networks, *Atmospheric Environment*, 45, 1337–1346, doi: 10.1016/j.atmosenv.2010.11.050, 2011.
- 1500 ~~Sparks, J. P., Monson, R. K., Sparks, K. L., and Lerdau, M.: Leaf uptake of nitrogen dioxide (NO₂) in a tropical wet forest: implications for tropospheric chemistry, *Oecologia*, 127, 214–221, doi:10.1007/s004420000594, 2001.~~
- Staelens, J., Houle, D. and De Schrijver, A., Neiryneck, J., and Verheyen, K.: Calculating Dry Deposition and Canopy Exchange with the Canopy Budget Model: Review of Assumptions and Application to Two Deciduous Forests, *Water, Air, and Soil Pollution*, 191, 149–169, doi:10.1007/s11270-008-9614-2, 2008.
- 1505 Sutton, M. A. and Fowler, D.: A Model for Inferring Bi-directional Fluxes of Ammonia Over Plant Canopies, in: Proceedings of the WMO conference on the measurement and modelling of atmospheric composition changes including pollutant transport, pp. 179–182, WMO/GAW (Global Atmosphere Watch)-91, Geneva, Switzerland, 1993.
- Sutton, M. A., Tang, Y. S., Miners, B., and Fowler, D.: A New Diffusion Denuder System for Long-Term, Regional Monitoring of Atmospheric Ammonia and Ammonium, *Water, Air and Soil Pollution: Focus*, 1, 145–156, doi:10.1023/a:1013138601753, 2001.
- 1510 Sutton, M. A., Howard, C. M., Erisman, J. W., Billen, G., Bleeker, A., Grennfelt, P., van Grinsven, H. and Grizzetti, B.: The European Nitrogen Assessment: sources, effects and policy perspectives, Cambridge University Press, Cambridge, UK, 2011.
- Sutton, M. A., Reis, S., Riddick, S. N., Dragosits, U., Nemitz, E., Theobald, M. R., Tang, Y. S., Braban, C. F., Vieno, M., Dore, A. J., Mitchell, R. F., Wanless, S., Daunt, F., Fowler, D., Blackall, T. D., Milford, C., Flechard, C. R., Loubet, B., 1515 Massad, R., Cellier, P., Personne, E., Coheur, P. F., Clarisse, L. Van Damme, M., Ngadi, Y., Clerbaux, C., Skjoth, C. A., Geels, C., Hertel, O., Wichink Kruit, R. J., Pinder, R. W., Bash, J. O., Walker, J. T., Simpson, D., Horvath, L., Misselbrook, T. H., Bleeker, A., Dentener, F. and de Vries, W.: Towards a climate-dependent paradigm of ammonia emission and deposition, *Philosophical Transactions of the Royal Society of London. Series B.: Biological Sciences*, 368, 20130166, doi: 10.1098/rstb.2013.0166, 2013.
- 1520 Tang, Y. S., Simmons, I., van Dijk, N., Di Marco, C., Nemitz, E., Dämmgen, U., Gilke, K., Djuricic, V., Vidic, S., Gliha, Z., Borovecki, D., Mitosinkova, M., Hanssen, J. E., Uggerud, T. H., Sanz, M. J., Sanz, P., Chorda, J. V., Flechard, C. R., Fauvel, Y., Ferm, M., Perrino, C., and Sutton, M. A.: European scale application of atmospheric reactive nitrogen measurements in a low-cost approach to infer dry deposition fluxes, *Agriculture, Ecosystems and Environment*, 133, 183–195, doi:10.1016/j.agee.2009.04.027, 2009.
- 1525 Tang, Y. S., Cape, J. N., Braban, C. F., Twigg, M. M., Poskitt, J., Jones, M. R., Rowland, P., Bentley, P., Hockenhull, K., Woods, C., Leaver, D., Simmons, I., van Dijk, N., Nemitz, E., and Sutton, M. A.: Development of a new model DELTA sampler and assessment of potential sampling artefacts in the UKEAP AGANet DELTA system: summary and technical report, Tech. rep., London, available at: https://uk-air.defra.gov.uk/library/reports?report_id=861 (last access: 22 July 2022),

2015.

- 1530 Tang, Y. S., Flechard, C. R., Dämmgen, U., Vidic, S., Djuricic, V., Mitosinkova, M., Uggerud, H. T., Sanz, M. J., Simmons, I., Dragosits, U., Nemitz, E., Twigg, M., van Dijk, N., Fauvel, Y., Sanz, F., Ferm, M., Perrino, C., Catrambone, M., Leaver, D., Braban, C. F., Cape, J. N., Heal, M. R., and Sutton, M. A.: Pan-European rural monitoring network shows dominance of NH_3 gas and NH_4NO_3 aerosol in inorganic atmospheric pollution load, *Atmospheric Chemistry and Physics*, 1, 875–914, doi:10.5194/acp-21-875-2021, 2021.
- 1535 Tarnay, L. W., Gertler, A., and Taylor, G. E.: The use of inferential models for estimating nitric acid vapor deposition to semi-arid coniferous forests, *Atmospheric Environment*, 36, 3277–3287, doi:10.1016/S1352-2310(02)00303-5, 2002.
- Thoene, B., Rennenberg, H., and Weber, P.: Absorption of atmospheric NO_2 by spruce (*Picea abies*) trees, *New Phytologist*, 134, 257–266, doi:10.1111/j.1469-8137.1996.tb04630.x, 1996.
- ~~Trebs, I., Metzger, S., Meixner, F. X., Helas, G., Hoffer, A., Rudich, Y., Falkovich, A. H., Moura, M. A. L., da Silva Jr., R. S., Artaxo, P., Slanina, J., and Andreae, M. O.: The $\text{NH}_4^+ - \text{NO}_3^- - \text{Cl}^- - \text{SO}_4^{2-} - \text{H}_2\text{O}$ aerosol system and its gas phase precursors at a pasture site in the Amazon Basin: How relevant are mineral cations and soluble organic acids?, *Journal of Geophysical Research: Atmospheres*, 110, doi:10.1029/2004JD005478, 2005.~~
- Ulrich, B.: Nutrient and acid-base budget of central European forest ecosystems, in: *Effects of Acid Rain on Forest Processes*, edited by: Godbold, D., and Hüttermann, A., John Wiley & Sons, New York, USA, 1–50, 1994.
- 1545 ~~UNECE: International Cooperative Program on Integrated Monitoring of Air Pollution Effects on Ecosystems (ICPIM) within the framework of the Geneva Convention on Long Range Transboundary, available at: <http://www.unece.org/env/lrtap/> (last access: 14 March 2022), 2022.~~
- ~~Van Damme, M., Clarisse, L., Franco, B., Sutton, M. A., Erisman, J. W., Wichink Kruit, R., van Zanten, M., Whitburn, S., Hadji-Lazaro, J., Clerbaux, C. and Coheur, P. F.: Global, regional and national trends of atmospheric ammonia derived from a decadal (2008–2018) satellite record, *Environmental Research Letters*, 16, 055017, doi:10.1088/1748-9326/abd5e0, 2021.~~
- 1550 Van der Graaf, S. C., Kranenburg, R., Segers, A. J., Schaap, M., and Erisman, J. W.: Satellite-derived leaf area index and roughness length information for surface–atmosphere exchange modelling: a case study for reactive nitrogen deposition in north-western Europe using LOTOS-EUROS v2.0, *Geoscientific Model Development*, 13, 2451–2474, doi:10.5194/gmd-13-2451-2020, 2020.
- 1555 Van Jaarsveld, J. A.: The Operational Priority Substances model. Description and validation of OPS-Pro 4.1., RIVM, Bilthoven, report 500045001, <https://www.pbl.nl/sites/default/files/downloads/500045001.pdf> (last access: 14 March 2022), 2004.
- Van Oss, R., Duyzer, J., and Wyers, P.: The influence of gas-to-particle conversion on measurements of ammonia exchange over forest, *Atmospheric Environment*, 32, 465–471, doi:10.1016/S1352-2310(97)00280-X, 1998.
- 1560 Van Pul, W. A. J. and Jacobs, A. F. G.: The conductance of a maize crop and the underlying soil to ozone under various environmental conditions, *Boundary-Layer Meteorology*, 69, 83–99, doi:10.1007/BF00713296, 1994.
- Van Zanten, M. C., Sauter, F. J., Wichink Kruit, R. J., van Jaarsveld, J. A., and van Pul, W. A. J.: Description of the DEPAC module; Dry deposition modeling with DEPAC_GCN2010, Tech. rep., RIVM, Bilthoven, NL, 2010.
- VDI: VDI-Guideline 3782 Part 5: Environmental meteorology – Atmospheric dispersion models – Deposition parameters, Tech. rep., Verein Deutscher Ingenieure, Düsseldorf, DE, 2006.
- ~~Walker, J. T., Beachley, G., Zhang, L., Benedict, K. B., Sive, B. C., and Schwede, D. B.: A review of measurements of air-surface exchange of reactive nitrogen in natural ecosystems across North America, *Science of The Total Environment*, 698, 133975, doi:10.1016/j.scitotenv.2019.133975, 2020.~~
- ~~Watson, L., Lacrosonnière, G., Gauss, M., Engardt, M., Andersson, C., Josse, B., Maréchal, V., Nyiri, A., Sobolowski, S., Siour, G., Szopa, S., and Vautard, R.: Impact of emissions and +2°C climate change upon future ozone and nitrogen dioxide over Europe, *Atmospheric Environment*, 142, 271–285, doi:10.1016/j.atmosenv.2016.07.051, 2016.~~
- 1570

- Webb, E. K.: Profile relationships: The log-linear range, and extension to strong stability, *Quarterly Journal of the Royal Meteorological Society*, 96, 67–90, doi:10.1002/qj.49709640708, 1970.
- 1575 Wentworth, G. R., Murphy, J. G., Benedict, K. B., Bangs, E. J., and Collett Jr, J. L.: The role of dew as a nighttime reservoir and morning source for atmospheric ammonia, *Atmospheric Chemistry and Physics Discussions*, 16, 1–36, doi:10.5194/acp-2016-169, 2016.
- Whitehead, J. D., Twigg, M., Famulari, D., Nemitz, E., Sutton, M. A., Gallagher, M. W., and Fowler, D.: Evaluation of laser absorption spectroscopic techniques for eddy covariance flux measurements of ammonia, *Environ Sci Technol*, 42, 2041–6, doi:10.1021/es071596u, 2008.
- 1580 Wichink Kruit, R. J., van Pul, W. A. J., Sauter, F. J., van den Broek, M., Nemitz, E., Sutton, M. A., Krol, M., and Holtslag, A. A. M.: Modeling the surface–atmosphere exchange of ammonia, *Atmospheric Environment*, 44, 945–957, doi:10.1016/j.atmosenv.2009.11.049, 2010.
- Wichink Kruit, R. J., Schaap, M., Sauter, F. J., van Zanten, M. C., and van Pul, W. A. J.: Modeling the distribution of ammonia across Europe including bi-directional surface–atmosphere exchange, *Biogeosciences*, 9, 5261–5277, doi:10.5194/bg-9-5261-1585 2012, 2012.
- Wichink Kruit, R. J., Aben, J., de Vries, W., Sauter, F. J., van der Swaluw, E., van Zanten, M. C., and van Pul, W. A. J.: Modelling trends in ammonia in the Netherlands over the period 1990–2014, *Atmospheric Environment*, 154, 20–30, doi:10.1016/j.atmosenv.2017.01.031, 2017.
- Wintjen, P., Ammann, C., Schrader, F., and Brümmer, C.: Correcting high-frequency losses of reactive nitrogen flux measurements, *Atmospheric Measurement Techniques*, 13, 2923–2948, doi:10.5194/amt-13-2923-2020, 2020.
- Wintjen, P., Schrader, F., Schaap, M., Beudert, B., and Brümmer, C.: Forest–atmosphere exchange of reactive nitrogen in a remote region – Part I: Measuring temporal dynamics, *Biogeosciences*, 19, 389–413, doi:10.5194/bg-19-389-2022, 2022.
- ~~Wolff, V., Trebs, I., Foken, T., and Meixner, F. X.: Exchange of reactive nitrogen compounds: concentrations and fluxes of total ammonium and total nitrate above a spruce canopy, *Biogeosciences*, 7, 1729–1744, doi:10.5194/bg-7-1729-2010, 2010.~~
- 1595 Wyers, G. and Duyzer, J.: Micrometeorological measurement of the dry deposition flux of sulphate and nitrate aerosols to coniferous forest, *Atmospheric Environment*, 31, 333–343, doi:10.1016/S1352-2310(96)00188-4, 1997.
- Wyers, G. P. and Erismann, J. W.: Ammonia exchange over coniferous forest, *Atmospheric Environment*, 32, 441–451, doi:10.1016/S1352-2310(97)00275-6, 1998.
- Zhang, L., Gong, S., Padro, J., and Barrie, L.: A size-segregated particle dry deposition scheme for an atmospheric aerosol module, *Atmospheric Environment*, 35, 549–560, doi:10.1016/S1352-2310(00)00326-5, 2001.
- 1600 Zöll, U., Brümmer, C., Schrader, F., Ammann, C., Ibrom, A., Flechard, C. R., Nelson, D. D., Zahniser, M., and Kutsch, W. L.: Surface–atmosphere exchange of ammonia over peatland using QCL-based eddy-covariance measurements and inferential modeling, *Atmospheric Chemistry and Physics*, 16, 11283–11299, doi:10.5194/acp-16-11283-2016, 2016.
- Zöll, U., Lucas-Moffat, A. M., Wintjen, P., Schrader, F., Beudert, B., and Brümmer, C.: Is the biosphere-atmosphere exchange of total reactive nitrogen above forest driven by the same factors as carbon dioxide? An analysis using artificial neural networks, *Atmospheric Environment*, 206, 108–118, doi:10.1016/j.atmosenv.2019.02.042, 2019.
- 1605